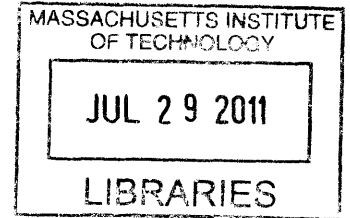


Path Planning Methods for Autonomous Underwater Vehicles

by
Konuralp Yiğit



Submitted to the Department of Mechanical Engineering
in partial fulfillment of the requirements for the degree of

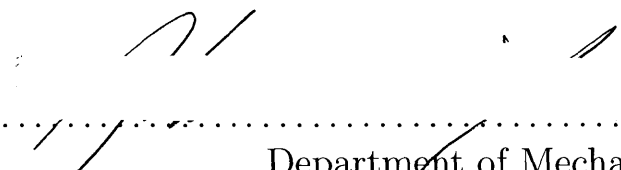
ARCHIVES

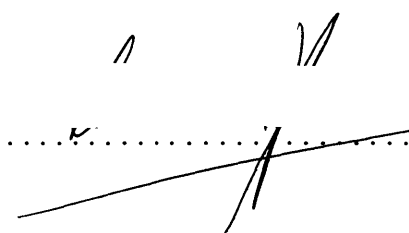
Master of Science in Naval Architecture and Marine Engineering
at the

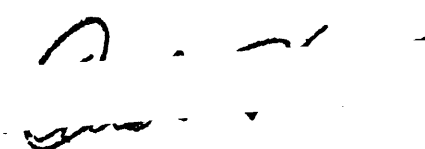
MASSACHUSETTS INSTITUTE OF TECHNOLOGY

June 2011

© Massachusetts Institute of Technology 2011. All rights reserved.

Author 
Department of Mechanical Engineering
May 6, 2011

Certified by 
Pierre F.J. Lermusiaux
Associate Professor
Thesis Supervisor

Accepted by 
David E. Hardt
Chairman, Department Committee on Graduate Theses

Path Planning Methods for Autonomous Underwater Vehicles

by

Konuralp Yiğit

Submitted to the Department of Mechanical Engineering
on May 6, 2011, in partial fulfillment of the
requirements for the degree of
Master of Science in Naval Architecture and Marine Engineering

Abstract

From naval operations to ocean science missions, the importance of autonomous vehicles is increasing with the advances in underwater robotics technology. Due to the dynamic and intermittent underwater environment and the physical limitations of autonomous underwater vehicles, feasible and optimal path planning is crucial for autonomous underwater operations. The objective of this thesis is to develop and demonstrate an efficient underwater path planning algorithm based on the level set method. Specifically, the goal is to compute the paths of autonomous vehicles which minimize travel time in the presence of ocean currents. The approach is to either utilize or avoid any type of ocean flows, while allowing for currents that are much larger than the nominal vehicle speed and for three-dimensional currents which vary with time. Existing path planning methods for the fields of ocean science and robotics are first reviewed, and the advantages and disadvantages of each are discussed. The underpinnings of the level set and fast marching methods are then reviewed, including their new extension and application to underwater path planning. Finally, a new feasible and optimal time-dependent underwater path planning algorithm is derived and presented. In order to demonstrate the capabilities of the algorithm, a set of idealized test-cases of increasing complexity are first presented and discussed. A real three-dimensional path planning example, involving strong current conditions, is also illustrated. This example utilizes four-dimensional ocean flows from a realistic ocean prediction system which simulate the ocean response to the passage of a tropical storm in the Middle Atlantic Bight region.

Thesis Supervisor: Pierre F.J. Lermusiaux
Title: Associate Professor

Acknowledgments

This thesis would not have been possible without the contributions and the help of members of Multidisciplinary Simulation, Estimation, and Assimilation Systems(MSEAS) group members who in one way or another contributed and extended their valuable contributions in the completion of this study.

First and foremost, my utmost gratitude to Professor Pierre J. F. Lermusiaux , Doherty Associate Professor in Ocean Utilization whose sincerity and encouragement I will never forget ! Literally speaking, he enabled me to develop wide perspective about scientific and engineering problems. I will always remember the great atmosphere he created in our research group ! I would also like to extend my special thanks to;

Dr. Patrick Haley, senior research scientist of MSEAS at MIT, who supprises me with his ingenuity every time we talk. It was not possible to finish this thesis without his clever contributions.

Dr. Themistoklis Sapsis, who is a post doctoral scientist of MSEAS at MIT, for giving me the chance of having deep intellectual and scientific discussions with him, and for his invaluable personal support.

Mattheus Ueckermann (S.M), who is a Ph.D Candidate of MSEAS at MIT, for his great help, invaluable discussions about this thesis work, and his great friendship during this study.

Dr. Wayne G. Leslie, who is a senior research scientist of MSEAS at MIT, for his patience and great support to complete this study;

Thomas Sondergaard, who is a S.M. Candidate of MSEAS at MIT, for our discussions, practical suggestions, and invaluable personal support.

Tapovan Lolla, who is a S.M. candidate of MSEAS at MIT, for his great help and clever ideas.

Mark S. Welsh, who is the Professor of Naval Practice and the Captain of U.S. Navy, for his great help and understanding.

Pete Small, who is the Associate Professor of Naval Practice and the Commander of U.S. Navy, for his help and understanding.

Leslie Regan, who is the manager of the Graduate Office of Mechanical Engineering Department at MIT, for her great understanding and help.

Ozge Karanfil, who is Ph.D candidate at Sloan School of Management of MIT, for her invaluable discussion of the language of this thesis and for her personal support and tolerance.

Oguzhan Uyar, who is S.M candidate of Electrical Engineering Department of MIT, for his great support to document this thesis work.

Office of Naval Research of United States Navy, for enabling us to work on this research project.

Turkish Navy, for enabling me to have this exciting research experience at MSEAS group of MIT.

Contents

1	Introduction	13
2	Review of Existing Methodologies	17
2.1	Introduction	17
2.2	Review of Other Methods	18
2.3	Level Set Method in Path Planning	22
2.4	Underwater Path Planning with Level Set and Fast Marching Methods	25
3	Level Set Method Theory	33
3.1	Introduction	33
3.2	Level Set Method	34
3.2.1	Formulation of Time-Dependent Front Evolution in the Normal Direction	34
3.2.2	Viscosity Solutions	36
3.2.3	Numerical Discretization of the Front Evolution in the Normal Direction	39
3.2.4	Front Evolution Due to Field Forces	42
3.2.5	Numerical Discretization of the Front Evolution due to Field Forces	42
3.2.6	Curvature-Driven Front Evolution	43
3.2.7	Putting Everything together	44
3.2.8	Construction and Reinitialization of the Signed Distance Field	46
3.3	Fast Marching Method	47

3.3.1	Introduction	47
3.3.2	Dijkstra Algorithm	48
3.3.3	Fast Marching Algorithm	49
3.3.4	Reinitialization of the Signed Distance Field with Fast Marching	51
3.4	Backward Calculations	51
4	Underwater Path Planning	53
4.1	Introduction	53
4.2	Algorithm	54
4.3	Applications and Test-Cases	55
4.4	Path Planning with Ocean Prediction System	63
5	Conclusions	67
5.1	Summary of Results	68
5.2	Suggestions and Future Work	69
A	Description of Matlab Files	71
A.1	Matlab Scripts for Two Dimensional Calculations	71
A.2	Matlab Scripts for Three Dimensional Calculations	72

List of Figures

2-1	Geodesic Path Planning (reprinted from (Sethian, 1999))	23
2-2	Robotic path planning with differential constraints (reprinted from (Kimmel and Sethian, 2001))	24
2-3	From left to right L1, L2, and L-infinity norms contours (reprinted from (Alton and Mitchell, 2009))	25
2-4	a) Isotropic b) Path planning in the presence of currents (reprinted from (Petres et al., 2007))	27
2-5	a) No field forces b) Path planning in the presence of currents (reprinted from (Petres et al., 2007))	28
2-6	Path planning with lifelong Fast Marching Method (reprinted from (Evans et al., 2008))	29
2-7	Level set contours without obstacles (reprinted from (Xu et al., 2009))	30
2-8	Path planning with detected obstacles (reprinted from (Xu et al., 2009))	31
3-1	Evolving circle (reprinted from (Sethian, 1996b))	35
3-2	Super and Sub-Differential of ϕ (reprinted from (Bressan and Piccoli, 2007))	38
3-3	Fast Marching Algorithm; red points represents set of accepted points, blue Points represents set of trial points	50
4-1	Test-Case 1	55
4-2	Test-Case 2	56
4-3	Test-Case 3	57
4-4	Test-Case 4	58

4-5	Test-Case 5	59
4-6	Boundaries of Lid-Driven Cavity Flow Domain	60
4-7	Time Dependent Lid-Driven Cavity Flow with front evolution	61
4-8	Test-Case 6	61
4-9	Test-Case 7	62
4-10	Ocean Flow Prediction on Near Surface level	63
4-11	Ocean Flow Prediction on Near Bottom level	64
4-12	3D Path Planning, red curve represents 3D Trajectory and other curves represent projections on cartesian planes	65

Nomenclature

Γ	Closed Interface Curve bounding a open region Ω
κ	Curvature of front
μ	Time of arrival function
∇	Gradient operator
Ω	Open region
\vec{n}	Normal vector
\vec{V}	Velocity vector of the front motion due to the field forces
\vec{V}_c	Velocity vector of the front motion due to the curvature
ϕ	Signed distance function
ϕ_t	Derivative of ϕ with respect to time
ϕ_x	Derivative of ϕ with respect to x
ϕ_y	Derivative of ϕ with respect to y
τ	Cost function
d	Distance from zero level set
D^+	Forward difference operator
D^-	Backward difference operator

D°	Central difference operator
H	Hamiltonian
p	Gradient of ϕ
T	Time of arrival function
V_n	Speed of front in the normal direction
X	Coordinate of point in domain Ω

Chapter 1

Introduction

The ocean is subject to a large set of forcing including atmospheric forcing (winds, sunlight, precipitation, etc), coastal forcing (rivers, glaciers, etc), and gravitational and earth forcing (rotation, seabed, tides, etc). Once oceanic motions are taking place, internal ocean dynamics lead to multiple features and possibly complex ocean currents. In order to carry out efficient and to best utilize or avoid the ocean currents, it is crucial to utilize ocean prediction from ocean models to compute optimal path for the ocean vehicles.

Ocean prediction and simulation systems are being used for ocean simulations and real-time forecasts of the ocean regions in shallow water regions to deep ocean regions, from the turbulent scales to climate scales. One of these ocean prediction system for regional coastal dynamics is the MIT Multidisciplinary Simulation, Estimation and Assimilation System (MSEAS) (Web-MSEAS, 2011), which is based on the Harvard Ocean Prediction System (HOPS) and includes many different computational and methodological tools such as the two-way nesting with free-surface dynamics and strong tidal forcing (Haley and Lermusiaux, 2010), the Error Subspace Statistical Estimation (ESSE) system for data assimilation (Lermusiaux, 1999), Dynamically Orthogonal Field Equations (Sapsis and Lermusiaux, 2009), Adaptive Sampling (Lermusiaux, 2007), Coupled Ocean-Acoustic Transmission Loss Prediction System (Lermusiaux et al., 2010).

Because of its predicting, simulating and real-time capabilities, MSEAS can be used as operational tool for underwater missions carried out by AUVs, such as adaptive sampling of the ocean variables, acoustic search missions for underwater warfare, underwater exploration and reconnaissance missions, One research project of the Multidisciplinary Simulation, Estimation and Assimilation System group at MIT is to develop new formalisms and methodologies for optimal marine sensing using collaborative swarms of autonomous platforms (AUVs, gliders, ships, moorings, remote sensing) that are smart, i.e. knowledgeable about the predicted environment, acoustic performance and uncertainties, and about the predicted effects of their sensing. This project is called A-MISSION - Autonomous Marine Intelligent Swarming Systems for Interdisciplinary Observing Networks. There is no doubt that path planning algorithms, which have a capability of handling the highly dynamic ocean environment, utilizing ocean models, and producing feasible and time/energy optimal paths, are very important part for the underwater missions. Investigating and employing methodologies for such path planning of ocean vehicles is the subject of the present research.

This thesis is focused on time optimal path planning problem of AUVs in dynamic ocean environment. This problem is solved with a new level set method based path planning algorithm. Together with the ocean predictions and simulations, this path planning algorithm can also produce feasible time optimal paths for underwater missions. One important novelty of this algorithm is that there is no need to define special anisotropic cost function for dynamic ocean environment as in (Petres et al., 2007). In addition to stated capabilities, our path planning algorithm can handle obstacles and bathymetry in the ocean environment without need of special implementation.

This thesis is organized as follows. Chapter 2 introduces the problem of path planning in dynamic ocean environment and reviews existing methodologies for path planning in dynamic ocean environments. Chapter 3 introduces the motivations for using level set method in path planning, and gives detailed background about level

set method and fast marching method. Chapter 4 shows the applications of the path planning algorithms. Examples test-case flows and MSEAS ocean model flows are used in this examples. Finally, Chapter 5 discusses future work and suggestions for path planning problem in dynamic ocean environments.

Chapter 2

Review of Existing Methodologies

2.1 Introduction

Researchers who are working on autonomous underwater vehicles path planning are increasingly addressing problems of insufficiency of path planning methods in the presence of ocean currents. These problems do not only require the consideration of energy or time optimal paths, but they also require the consideration of infeasible paths. Even though there are well-worked path planning algorithms in robotics research, assumptions that are necessary for incorporating the dynamic nature of the ocean into the path planning algorithms can cause infeasible solutions. For example, in the presence of strong currents, many path planning heuristics give infeasible solutions. Until now, traditional robotics methods have only provided approximate solutions which do not utilize the predictions of ocean currents in time and space. In this thesis, we will show that new level set methods derived by our MSEAS group are capable of accounting for these complex currents. Importantly, they can provide exact solutions to the time-optimal path planning problem in a limited number of computations that grow linearly with the number of vehicles and only geometrically in space.

The level set method is a numerical technique to track and simulate any kind of front and interface evolution. By using the level set method, one can perform

numerical analysis and simulations involving curves, surfaces, or higher dimensional objects on a fixed Cartesian grid without having to parameterize these objects as in Lagrangian approaches. (Osher and Fedkiw, 2001). In addition to that, the level set and fast marching methods provide an efficient and tractable framework for solving Eikonal and Hamilton Jacobi Equations by which time and energy optimal paths are produced. However, much care must be taken to produce a feasible and optimal path planning solution in the presence of time-dependent forces, such as currents or moving obstacles. Applications to underwater vehicles, which are operated in the time varying ocean flow field, are highly limited at present.

This chapter explores the existing path planning methodologies for autonomous underwater vehicles. The main focus is on level set and fast marching method based path planning algorithms. However, we will also concisely review the existing methodologies other than level set based approaches. The organization of this chapter is as follows; Section 2.2 is a concise review of the existing methodologies of time/energy optimal path planning in ocean environments. In section 2.3, we review the existing level set and fast marching based ocean path planning algorithms. The reliability of the methodologies is discussed, and approaches for incorporating ocean flow dynamics into path planning algorithms are outlined.

2.2 Review of Other Methods

Path planning methods coupled with ocean prediction systems, which utilize the search method based on the Darwinian theories of natural selection, are proposed in (Alvarez et al., 2004), (Kanakakis and Tsourveloudis, 2007), and (Yang and Zhang, 2009). In the first study, which utilizes the method called genetic algorithms, feasible paths are iteratively transformed by evolutionary operators such as inheritance, crossover, selection, and mutation. For the path planning in time-varying ocean environment, they incorporate dynamic programming into their genetic algorithm based approach and propose a hybrid model. The second study is focused on feasible and

safe trajectory generation, but the presence of strong ocean currents is not taken into account. A fuzzy controller for the trajectory correction, which utilizes the measurements taken by AUV, during the AUVs operation is proposed. In the third study, in order to find energy optimal and feasible paths, the method called particle swarm optimization is adapted. A new algorithm, called adapted inertia-weight particle swarm optimal algorithm, is proposed to speed up the process of convergence to the global minimum.

Another approach for path planning coupled with relatively simple ocean prediction, which utilizes graph search techniques, are proposed by (Carroll et al., 1992) , (Garau et al., 2005) . In the first study, an A* approach graph search technique is utilized for path planning. The proposed algorithm is constrained with two dimensional case, and no ocean prediction system data is incorporated into applications. In the second study, path planning in terms of the spatial scales of ocean variability is investigated. As in previous study, A* graph search technique is used. One advantage comparing to the previous A* approach is that the performance is increased by incorporating heuristics into the algorithm and the energy optimality is considered. In order to achieve this goal, time optimal trajectories are computed by using ocean basins simulations with different eddy sizes and current speeds. Therefore, the existence of a heuristic to guide the A* search procedure and its dependence on the ocean current structure is analyzed. The main drawbacks of the second study are stated as follows; in the second study, the currents are assumed to be time-independent and two dimensional. The vehicle trajectories are constrained to grid points, and must be in the direction of cartesian axes, and A* algorithm is highly susceptible to the curse of dimensionality.

A different approach is proposed by (Soulignac et al., 2009) . This study is mainly focused on path planning in the presence of strong ocean currents (Higher ocean current speed than vehicle speed) and use the method called wavefront expansion (Dorst and Trovato, 1988) . They defined a new cost function in order to find feasible

paths in the presence of strong ocean currents. The limitation of this approach is that their cost function cannot handle the variable vehicle speed cases. Another approach, which utilizes the potential field theory from robotics together with the evolutionary optimization approach, is proposed by (Witt and Dunbabin, 2008). In this study, time versus energy optimality tradeoff is made for the AUVs operations. Together with the real-time experiments, local and global optimization methods are investigated. However, the time-varying nature of the ocean flow is not considered, and ocean flow speed is assumed to be time-independent.

An interesting approach proposed by (Vasudevan and Ganesan, 1996) which is based on case-based reasoning and aims to produce feasible trajectories for AUVs. Case-based reasoning is a computational method that utilizes the previous experiences, gathered knowledge, and calculated data to produce solutions to the problems. In this study, the proposed scheme produces trajectories by modifying old trajectories or by synthesizing the acquired experiences with planned trajectories in the operation region. Another approach using case-based reasoning, which is not directly focused on underwater path planning, is proposed by (Kruusmaa, 2003) . In this study, in addition to the previous study, time-optimal trajectories in the presence of dynamic obstacles are also considered. Even though case-based reasoning approach can be quite useful in known and well-studied regions, it can hardly be practical in poorly-studied regions or in the presence of time-constraints, such as naval operation conditions.

An elegant control theoretic approach for path planning problem for AUVs is proposed by (Inanc et al., 2005). The basic idea of this study is to utilize lagrangian coherent structures in the ocean currents to produce near-optimal paths for gliders. The path planning problem is formulated as standard constrained (both in state and control) optimal control problem, and the near-optimal trajectories are obtained by transcribing the problem into nonlinear optimization problem (NLP), and then solving it with NLP methods. Another control theoretic study, which is focused on

lagrangian coherent structures, is proposed by (Zhang et al., 2008). This study is focused on 2 dimensional flows on ocean and the near optimal trajectory solutions are produced by B-spline approach. B-splines are member of dynamic splines and useful approach to produce solutions in control theory, especially in trajectory generation problems (Kano et al., 2003). An interesting control theoretic approach, which presents feedback control strategy and utilizes lagrangian coherent structures, is proposed by (Senatore and Ross, 2008). In this study, the energy optimal trajectories are considered and 2 dimensional solutions are presented.

Application of well known robotics path planning algorithm, Rapid-Exploring Random trees (RRTs), to the underwater path planning for feasible and obstacle free trajectories is introduced by (Tan et al., 2004). RRTs has been widely used in robotic path planning, and it can efficiently find obstacle free paths even in the presence of dynamic obstacles (LaValle, 2006). A heuristic based approach, which is focused on positional uncertainties during AUVs operations, is introduced by (Smith et al., 2010). In this study, dead-reckoning error for Slocum gliders is calculated, and then the mean positional error recorded from multiple deployments conducted previously are compared with these calculations. Then, by using these experiences, a path planning algorithm is produced.

In this section, we have reviewed the different approaches for the path planning in underwater environment. These approaches can produce solutions for many different problems encountered by the underwater path planners. However, especially, because of dynamic nature of the underwater environment and limited computational sources in practical situations, it is difficult to present a full-fledged trajectory generation algorithm for underwater path planning. Level set and fast marching methods, which are main focus of this thesis, are two of the promising candidates that can cope with these difficulties for AUVs operations. In the next sections, we will review the approaches based on level set and fast marching methods.

2.3 Level Set Method in Path Planning

The level set method, which is introduced by (Osher and Sethian, 1988), is a framework for the computation of evolving fronts using implicit functions. Its key idea is to represent interfaces with continuous functions. The evolution of interfaces can be formulated as a signed distance Hamilton-Jacobi equation and computed with level set method. The first decade after its invention, with the invention of Dijkstra shortest path like algorithm, which is called fast marching (Tsitsiklis, 1995), the level set and the fast marching methods started to play a role in continuous time and space path planning of autonomous vehicles. Especially, because of its built-in fast and optimal computation time, fast marching method has gotten important role in autonomous robotic path planning. Our research group has also recently developed new schemes based on level set and fast marching methods for the mapping of gappy ocean data in complex multiply-connected coastal regions (Agarwal, 2009) and (Lermusiaux et al., 2011).

The Fast marching method is a numerical solution method for solving the Eikonal equation on a cartesian orthogonal grid reference. The fast marching scheme hinges on an upwind numerical approach to the gradient of the Eikonal equation. The fast marching method is strongly connected to Fermat's principle of least time, which is a construction through evolving wavefront, and Dijkstra's shortest path algorithm, which is a computational method to calculate global optimum path in graphs or cartesian orthogonal grid domains (Sethian, 1996b). The fast marching solutions gives us optimal arrival times contours in the orthogonal domain from which time optimal solution of paths are easily obtained. In this section, we discuss level set and fast marching methods based path planning algorithms. First, we concisely discuss path planning methods in the robotics area, and then we will focus on existing work related to AUVs. The technical detailed information about level set method and fast marching method is given in Chapter-3.

Fast marching algorithm for continuous trajectory optimization and planning is first introduced by (Tsitsiklis, 1995). In his seminal paper, Tsitsiklis introduces a continuous version of the Dijkstra-like algorithm and solves it with a semi-lagrangian approach. He gives examples from obstacles avoidance and shortest path planning in 2 dimensional static configuration spaces. One year later, in the seminal paper of Sethian (Sethian, 1996a), it is shown that the fast marching algorithm together with the upwind difference methods satisfies the viscosity solutions of the Eikonal equation. In (Kimmel and Sethian, 1998), a different discretization approach is proposed, called triangulated fast marching algorithm, for the fast marching algorithm which enables the path planning on manifolds. Please see Figure 2-1 below. Therefore, thanks to these two important studies, the fast marching and the level set methods became important path planning tools in robotics path planning.

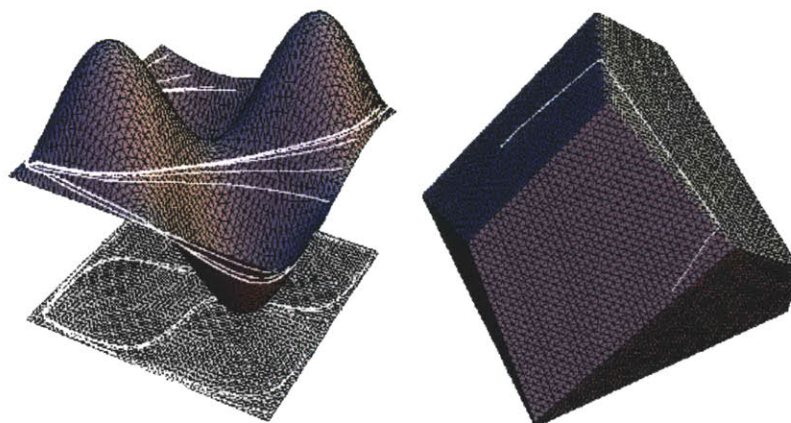


Figure 2-1: Geodesic Path Planning (reprinted from (Sethian, 1999))

Two years later, in the work of (Kimmel and Sethian, 2001), the robotics path planning in the presence of differential constraints was introduced. Therefore, the fast marching approach became no longer constrained to point body dynamics, and it becomes practical tool in path planning for robotics. Please see Figure 2-2. Another very important step in path planning by using anisotropic approach, based on fast marching method, is proposed in (Sethian and Vladimirsky, 2000). This has special

importance for underwater path planning because no isotropic approach can represent the nature of dynamic ocean environments.

Variational calculus based approaches in level set methods were first introduced by (Zhao et al., 1996). The application of path planning based on variational level set method is proposed in (Cecil and Marthaler, 2006). In this study, they consider the problem of producing a search path for finding targets, in the presence of uncertainty. The goal is to find a optimum (shortest) and confident trajectories for target search. In their second paper (Cecil and Marthaler, 2006), they extend their previous 2 dimensional work to a 3 dimensional framework. They also use codimension-2 solutions for level set evolution and reinitialization schemes.

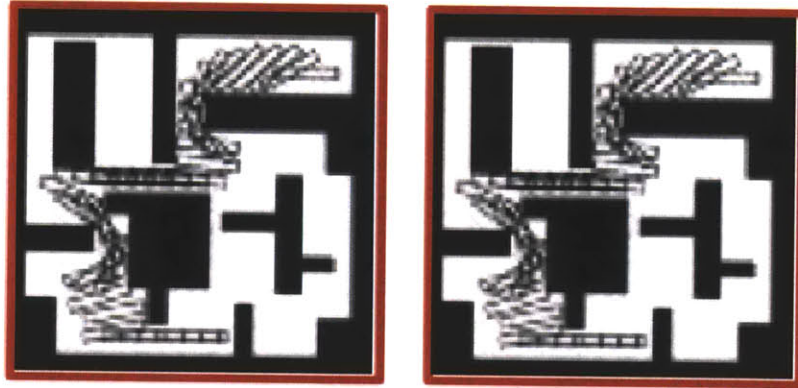


Figure 2-2: Robotic path planning with differential constraints (reprinted from (Kimmel and Sethian, 2001))

A different perspective to anisotropic path planning problems is proposed by (Alton and Mitchell, 2009). In this study, a new class of static Hamilton-Jacobi Partial differential equation with axis-aligned anisotropy is described. On orthogonal grids, this anisotropic static Hamilton-Jacobi equation satisfies the causality condition requirement for standard finite-difference schemes and can therefore be solved using the fast marching method. They also present variations of Eikonal equation which use

L1, L2, and L-infinity norms on orthogonal grid domains of varying node spacing and arbitrary dimension. See Figure 2-3.

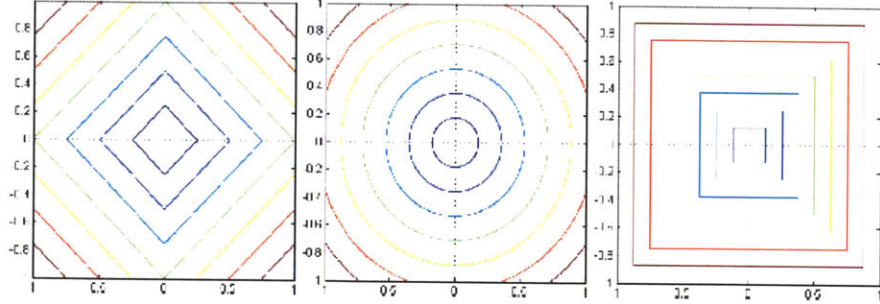


Figure 2-3: From left to right L1, L2, and L-infinity norms contours (reprinted from (Alton and Mitchell, 2009))

Today, researchers of robotics and image processing areas are increasingly incorporating level set and fast marching based approaches based approaches into path planning algorithms. With the increasing developments in mathematical techniques and computer technology, there is no doubt that these approaches will continue to stay as one of the main focus of the researchers. Because of the huge potential of the studies in robotics and image processing fields for the underwater path planning, the researchers, who are working on underwater path planning, should carefully follow developments in these fields. In the next section, we will review the path planning algorithms for AUVs based on level set and fast marching methods.

2.4 Underwater Path Planning with Level Set and Fast Marching Methods

Due to the highly dynamic nature of the sea, underwater path planning needs anisotropic cost functions. An anisotropic approach for underwater path planning using fast marching method was first introduced by (Petres et al., 2007) . The important aspects of this proposed anisotropic approach are that the curvature of the

final trajectory is constrained, which makes it possible to take differential constraints into account; new quadratic upwind finite difference scheme is developed. Therefore, directional constraints, such as ocean currents, can be taken into account. In order to handle the real-time constraints of underwater path planning and to speed up the computation time, multi-resolution grid system is applied to the new quadratic upwind difference scheme.

Basically, the proposed algorithm of (Petres et al., 2007) hinges on solving the Eikonal equation with anisotropic cost function τ . The cost function τ can be thought as the slowness of the vehicle at each point in the domain. The Eikonal equation together with the anisotropic cost function τ is stated as follows;

$$\|\nabla\mu\| = \tau \quad (2.1)$$

where $\mu : \Omega^2 \rightarrow \mathfrak{R}_+$ is distance function to minimize, and τ is dependent on the field force (currents) \vec{U} .

In order to handle currents, anisotropic cost function τ is split into two parts as in Equation-2.2. The first right hand term of the Equation-2.2 handles the isotropic constraints on the solution domain, and the second right hand term handles the anisotropic cost function that handles forces of the solution domain, such as ocean currents. τ_{obst} can be seen as standard isotropic cost function as in isotropic fast marching method. The details about isotropic cost function in fast marching method are given in Chapter-3. The anisotropic part of the cost function τ proposed by Petres et al is stated in Equation-2.3.

$$\tau = \tau_{obst} + \tau_{vect} \quad (2.2)$$

$$\tau_{vect}(i, j) = \alpha \left(1 - \frac{\langle \nabla\mu_{i,j}, \vec{U}_{i,j} \rangle}{Q_{i,j}} \right) \quad (2.3)$$

where $Q_{i,j} = (\tau_{abst}(i, j) + 2\alpha)sup_{\Omega}||\vec{U}||$ is a normalization term, and the α represents the gain. Basically, the second term of the cost function τ_{vect} means that fields forces, such as the ocean currents, favor the vehicle propulsion when they are in the same direction.

As it can be seen from Equation-2.3, the proposed cost function is insufficient to handle nonlinear reaction of the underwater vehicles to ocean currents. Examples are given only for the linear reaction cases. Please see Figure 2-4 and 2-5. Another limitation of this approach is that it can not cope with ocean fields in which ocean currents have higher velocity than underwater vehicle's velocity (Soulignac et al., 2008). In addition to this, (Petres et al., 2007) mention neither any utilization of the ocean prediction system nor the applicability of their approach to the ocean model domains.

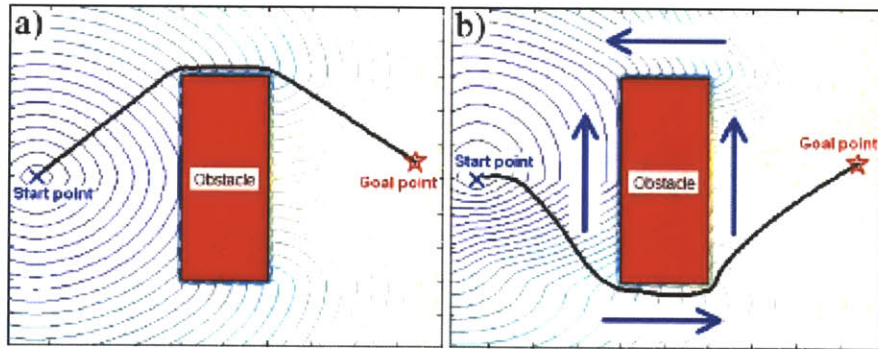


Figure 2-4: a) Isotropic b) Path planning in the presence of currents (reprinted from (Petres et al., 2007))

Another approach, which focuses on collision avoidance and utilizes the work of (Petres et al., 2007), is proposed by (Evans et al., 2008). This study is composed of three parts (layers). These are the sensor layer, scenario layer, and reactive layer. The

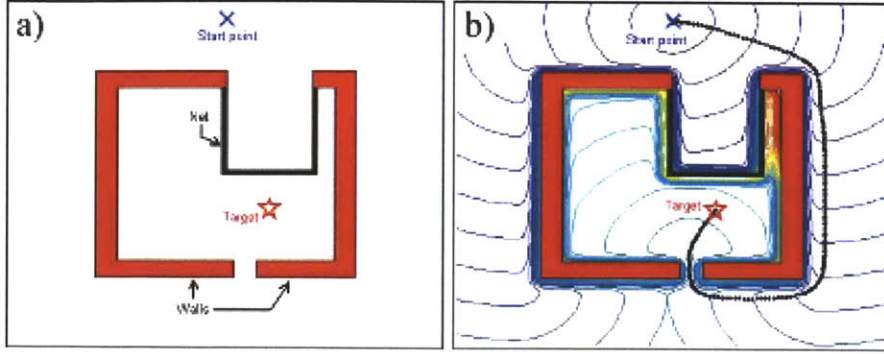


Figure 2-5: a) No field forces b) Path planing in the presence of currents (reprinted from (Petres et al., 2007))

main function of the sensor layer is to generate a local map of the operation field and to feed the scenario layer. The Scenario layer takes these local maps and incorporate these local maps in its previously programmed scenarios to produce feasible collision free paths. The reactive layer utilizes the fuzzy information coming from sensor and the scenario layers to generate safe paths in case of dire emergency conditions.

The gradient of the cost function is calculated by utilizing approach of (Petres et al., 2007), and the cost function throughout the domain is defined as in Equation-2.4.

$$\mu = \min \int_0^L \tau(C(s)) ds \quad (2.4)$$

where C represents all the trajectories that connect start point to destination point in domain, and τ is the cumulative cost of these trajectories with length L . Therefore, the Eikonal equation relating to the cost function stated in Equation-2.4 is given as in Equation-2.5.

$$|\nabla \mu| = \tau \quad (2.5)$$

In the solution approach, (Evans et al., 2008) extended the fast marching algorithm by incorporating heuristics from A* algorithm and incremental search methods from lifelong planning adapted from (Koenig et al., 2004). This new extended algorithm is called Lifelong Planning Fast Marching (LPFM*). One practical result produced by this algorithm is that when the configuration space, which is mapped onto local maps, is modified by the sensor layer, there is no need for re-calculation of the path while AUV is operating. Trajectory generator of this approach re-utilizes previous calculations, and calculations are needed to be carried out just for modified region. Examples from (Evans et al., 2008) are given in Figure 2-6.



Figure 2-6: Path planning with lifelong Fast Marching Method (reprinted from (Evans et al., 2008))

A level set based approach for the path planning is proposed by (Xu et al., 2009). The aim of this proposed approach is to propose a minimum risk trajectory planning method that relaxes the computational cost of path planning based on level set method in case of new obstacle detection while operating AUVs. This approach does not consider dynamics of the vehicle. It is assumed that collision risks in the operation region are detected by on-board limited range sensors. At every grid point, the cost function, which drives motion of the front in the normal direction, is defined according to the probability that indicates the risk of collision.

In this work, the computational cost of the path planning algorithm is reduced with two ways. First, it is assumed that if there is no risk of collision, previously planned trajectories remains optimal. Second, if an obstacle that creates risk of collision is detected, level set solution is only re-produced for this portion of the domain, and it is shown that this still gives optimal collision free trajectories. Underwater environments, such as riverine systems, are the main motivation of this work, and examples are given in Figure 2-7 and 2-8 .

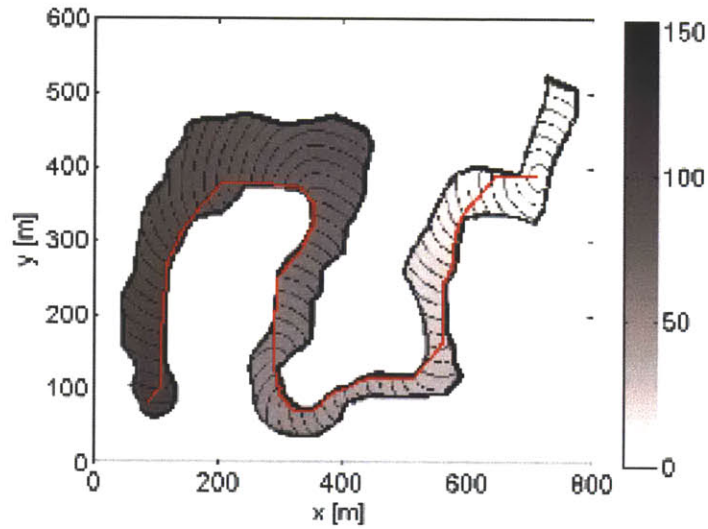


Figure 2-7: Level set contours without obstacles (reprinted from (Xu et al., 2009))

An elegant utilization of level set and fast marching methods for the objective analysis of ocean fields was developed by Multidisciplinary Simulation, Estimation and Assimilation System group at MIT, and it is proposed in (Agarwal, 2009). Objective analysis is a method to create a set of consistently gridded ocean fields from sparse observations (Bretherton et al., 1976). In this study, fast marching and level set methods are utilized for the estimation of length of optimal shortest sea paths to develop novel objective analysis scheme for complex coastal regions and archipelagos (chain or cluster of islands). A novel fast marching method based approach for estimation of

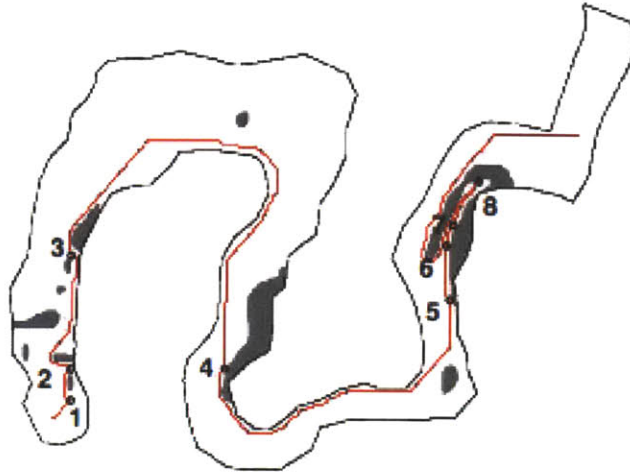


Figure 2-8: Path planning with detected obstacles (reprinted from (Xu et al., 2009))

absolute velocity under geostrophic balance in complex, multiply-connected coastal domains is presented. It is also demonstrated that proposed approach is more efficient and accurate than stochastically forced differential equations approach.

This section has reviewed the existing art related to the underwater path planning for AUVs. Underwater path planning other than level set based approaches and level set based path planning approaches for robotics and image processing are introduced in the sub-sections 2.2 and 2.3. The studies reviewed here were selected because of their contributions to the underwater path planning and the fact that they exploit the stated methods, such as genetics algorithms, etc., in an interesting and unique way.

The writer of this thesis believes that level set framework for the path planning in an ocean like environments has promising potential for the future. Even though the introduced techniques for the level set based path planning in this section have some important disadvantages, the level set based approach has a huge potential for being one of the best methodology for the path planning in an ocean-like environments, and as it is stated before, one objective of this thesis is to contribute to this.

The future use of level set based path planning in control of autonomous underwater vehicles is tied fundamentally to general advances in mathematical theory and computer technology. Due to the large mathematical nature of the level set based path planning, developments that arise in applied mathematics in one area are likely to provide benefits to the level set based path planning. The continued progress in computer technology and applied mathematical techniques will permit further realization of the level set based path planning. A challenge in ocean-like 4D environments is the large amount of computational-time required to reach a desired solution. On the other hand, the increasing availability of cheap, high-performance computing tools, coupled with advancements in mathematical techniques, will undoubtedly provide great benefit. In addition to increasing the effectiveness of the technique for level set based path planning techniques, developments in the field of applied mathematics should also make new level set based path planning methods for an ocean like environments possible, such as the narrow-band level set method (Adalsteinsson and Sethian, 1995), semi-lagrangian fast marching algorithms for optimal control, which is called Buffered Fast Marching Method (Cristiani, 2009), and the stochastic formulation of the level set method and its combination with filtering algorithms, such as (Osher and Paragios, 2003), (Soner and Touzi, 2002), and (Paragios and Deriche, 2002).

Chapter 3

Level Set Method Theory

3.1 Introduction

The aim of this chapter is to provide an introduction to the theory used in this thesis, and the theory of the level set method in particular. Level set method is a computational technique to simulate the evolution of the interfaces and is an approximation of solutions to the Hamilton-Jacobi type partial differential equations. It was first introduced by Osher and Sethian (Osher and Sethian, 1988). It can easily simulate the changing topology of the interfaces by parameterizing this interfaces in a higher dimensional space. It has been applied to many different fields such as fluid mechanics (Sussman and Puckett, 2000), computer graphics (Malladi et al., 1995), applied physics (Ki et al., 2001), geosciences (Agarwal, 2009), (Lermusiaux et al., 2011), and (Gout and Guyader, 2006), and robotics (Hassouna et al., 2005). In level set context, there are two different formulation of interface evolution. First formulation is the initial value formulation which is known as the classical level set method, and the second formulation is boundary value formulation which is known as the fast marching method. We will begin our discussion with classical level set method, and then fast marching method will be discussed. The discussion in this chapter is based on (Osher and Fedkiw, 2003)

3.2 Level Set Method

3.2.1 Formulation of Time-Dependent Front Evolution in the Normal Direction

The Eulerian approach proposed by level set methodology is to embed evolving fronts as zero level set of a N dimensional function ϕ to represent the motion of $N-1$ (co-dimension 1) dimensional hypersurface. For the 2 dimensional case, let $\phi(x, y, t = 0)$, where (x, y) defines the grid locations in 2 dimensional space.

$$\phi(x, y, t = 0) = \pm d \quad (3.1)$$

where d is the distance from zero level set $\Gamma(t = 0)$. The sign in front of the d is negative if the grid location (x, y) is inside the initial zero level set $\Gamma(t = 0)$, and opposite otherwise. Therefore, the initial function $\phi(x, y, t = 0) : R^2 \rightarrow R$ has a property on the interface that

$$\Gamma(t) = (x, y) : \phi(x, y, 0) = 0 \quad (3.2)$$

where Γ represents the closed interface curve bounding a open region Ω , ϕ is known as the signed distance function, and ϕ is assumed to take negative values inside the bounded region, and positive values outside the bounded region, and these are represented by Ω^- and Ω^+ respectively. Therefore, the signed distance function on the level set solution domain has the following properties.

$$\begin{aligned} \phi(x, y, t) < 0 & \quad \text{for } (x, y) \in \Omega^- \\ \phi(x, y, t) > 0 & \quad \text{for } (x, y) \in \Omega^+ \\ \phi(x, y, t) = 0 & \quad \text{for } (x, y) \in \Gamma(t) \end{aligned}$$

Now, the goal is to come up with an equation to represent evolving function $\phi(x, y, t)$ which includes the embedded evolution of the $\Gamma(t)$ as the zero level set of ϕ . In order to match the zero level set of the evolving function ϕ with the propagating front Γ , we must have

$$\phi(x, y, t) = 0 \tag{3.3}$$

and by the chain rule

$$\phi_t + \nabla\phi(x, y, t) \cdot X'(t) = 0 \tag{3.4}$$

where $X(t)=(x(t),y(t))$, Since unit normal vector to the evolving front is defined as $\vec{n} = \frac{\nabla\phi}{|\nabla\phi|}$, and $V_n(X(t)) = X_t \cdot \vec{n}$, given $\phi(X, t = 0)$, the evolution equation, also known as level set equation, can be written as

$$\phi_t + V_n|\nabla\phi| = 0 \tag{3.5}$$

Since the domain coordinate system is fixed, this solution is known as the Eulerian formulation of the front propagation. See Figure 3-1 for the demonstration evolving circle.

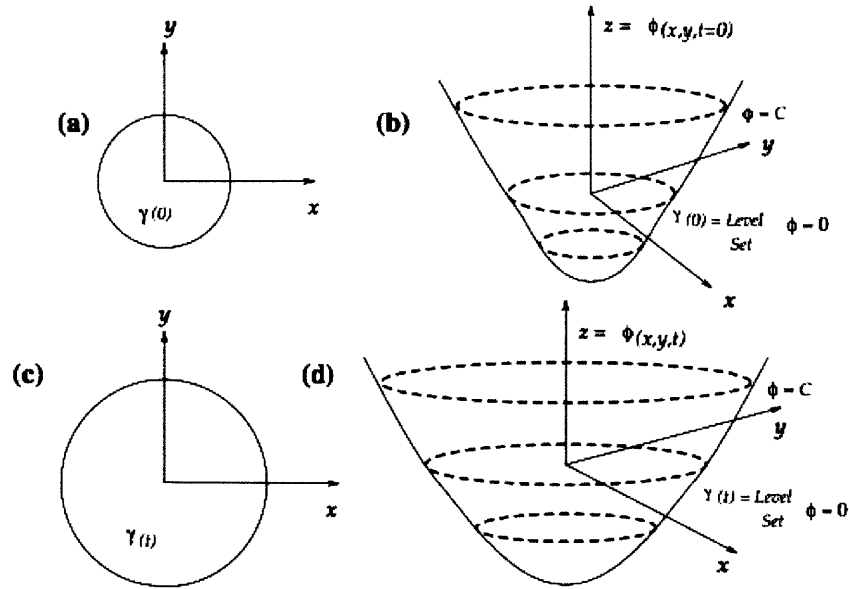


Figure 3-1: Evolving circle (reprinted from (Sethian, 1996b))

The major advantages of the level set formulation can be stated as follows

- First, if $V_n(X(t))$ is a smooth function, the evolving function $\phi(X, t)$ remains signed distance function. In spite of this, as the zero level set evolves $\phi = 0$ can change its topology, form corners, etc.
- Second, since the evolving $\phi(X, t)$ remains as a function, a finite difference approximation can be used to compute the evolving ϕ .
- Third, the intrinsic properties of the evolving front can easily be calculated using a level set function ϕ . For instance, the normal vector to the evolving front and curvature of the each level are respectively given by Equations 3.6 and 3.7.
- Fourth, the level set approach can easily be extended to represent evolving 3 dimensional fronts by just making straightforward extensions to gradient operators and the array structures.

$$\vec{n} = \frac{\nabla\phi}{|\nabla\phi|} \tag{3.6}$$

$$\kappa = \nabla \cdot \frac{\nabla\phi}{|\nabla\phi|} = \frac{\phi_{xx}\phi_y^2 - 2\phi_x\phi_y\phi_{xy} + \phi_{yy}\phi_x^2}{(\phi_x^2 + \phi_y^2)^{\frac{3}{2}}} \tag{3.7}$$

3.2.2 Viscosity Solutions

Since the numerical solution techniques of the level set method are based on viscosity solutions of Hamilton-Jacobi equations, we will briefly introduce viscosity solutions before discussing numerical approximation for the normal motion of the fronts. The viscosity solution concept was first proposed by (Crandall and Lions, 1983). The viscosity solution concept is a mathematical approach to solve a certain class of PDEs, which is of the form of $F(x, \phi, \nabla\phi, \nabla^2\phi) = 0$, and the function ϕ needs not be everywhere differentiable. Even if there are points where $\nabla\phi$ or $\nabla^2\phi$ does not exist, the

viscosity solutions satisfy the given properties of the PDE, and it gives solution to the given PDE. Therefore, uniqueness and existence theorems hold. In addition to that, viscosity solution concept leads to stable numerical solutions of the given PDE. It has especially been applied to PDEs arising in optimal control and differential games, where continuous solutions do not exist (Fleming and Soner, 2006). Since, in our path planning framework, we are interested in solving the first order Hamilton-Jacobi type equations, our objective PDE takes the form of Equation 3.8.

$$F(x, \phi, \nabla\phi) = 0 \quad x \in \Omega \subseteq \mathfrak{R}^n \quad (3.8)$$

One of the best known approaches to solve the PDEs of the form of Equation 3.8 is the method of characteristics. However, local smooth solutions produced by this technique cannot be applied to whole solution domain Ω . In fact, singularity occurs if the two or more characteristic front coincide at the same point on the domain Ω (Giga, 2006)

Even though the function ϕ is not continuous or differentiable over the entire domain, we can solve Equation 3.8 by utilizing the viscosity solution technique. Let $\varepsilon \rightarrow 0+$. The idea of the viscosity solution technique is that the solutions ϕ_ε of the parabolic PDE problem of the form of the equation below converge to a unique limit of ϕ (Crandall et al., 1992).

$$F(x, u_\varepsilon, \nabla\phi_\varepsilon) = \varepsilon\Delta\phi_\varepsilon \quad (3.9)$$

At each point on the domain where ϕ exists, characterization of the limit function ϕ can be made by applying certain inequalities on its super and sub-differentials. See Figure 3.1. On the open set $\subseteq \mathfrak{R}^n$, let $\phi : \rightarrow \mathfrak{R}$ be a scalar function and the $p \doteq \nabla\phi$. The super-differential and sub-differential sets of ϕ at the point X is defined as in the Equation 3.10 and 3.11 respectively (Bressan and Piccoli, 2007).

$$D^+ \phi(X) = \left(p \in \mathfrak{R}^n; \limsup_{Y \rightarrow X} \frac{\phi(Y) - \phi(X) - p \cdot (Y - X)}{|Y - X|} \leq 0 \right) \quad (3.10)$$

$$D^- \phi(X) = \left(p \in \mathfrak{R}^n; \liminf_{Y \rightarrow X} \frac{\phi(Y) - \phi(X) - p \cdot (Y - X)}{|Y - X|} \geq 0 \right) \quad (3.11)$$

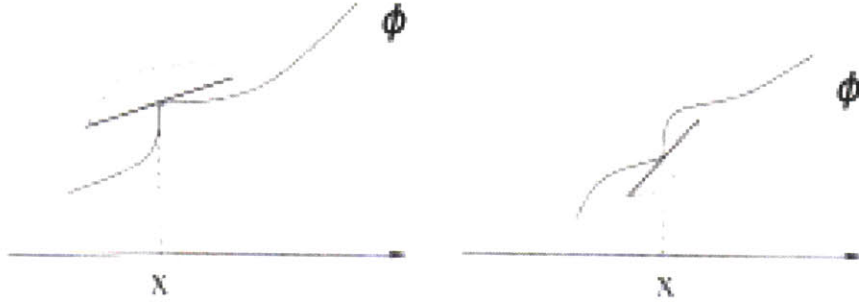


Figure 3-2: Super and Sub-Differential of ϕ (reprinted from (Bressan and Piccoli, 2007))

Namely, for every point $X \in \Omega$ and $p \in D^+ \phi(X)$, the function ϕ is a viscosity subsolution of the Equation 3.8 if $F(X, \phi(X), p) \leq 0$, and for every point $X \in \Omega$ and $p \in D^- \phi(X)$, the function ϕ is a viscosity subsolution of the Equation 3.8 if $F(X, \phi(X), p) \geq 0$.

Since we are interested in the time-dependent formulation of the front evolution, we define Hamiltonian $H = H(X, \phi, \nabla \phi, t)$. Note that second term $V_n |\nabla \phi|$ of the Equation 3.5 is of this type.

$$\phi_t + H(X, \phi(X), \nabla \phi, t) = 0 \quad (3.12)$$

Therefore, by applying similar definitions stated above to the Equation 3.12, we obtain the following statements;

- If for every point $X \in \Omega$, a function $\varphi = \varphi(X, t)$ such that $\phi - \varphi$ has a relative minimum at (X, t) , the function ϕ is a viscosity super-solution of Equation 3.12. Therefore, Equation 3.13 holds

$$\varphi_t + H(X, \phi, \nabla\varphi, t) \geq 0 \quad (3.13)$$

- If for every point $X \in \Omega$, a function $\varphi = \varphi(X, t)$ such that $\phi - \varphi$ has a relative maximum at (X, t) , the function ϕ is a viscosity sub-solution of Equation 3.12. Therefore, Equation 3.14 holds

$$\varphi_t + H(X, \phi, \nabla\varphi, t) \leq 0 \quad (3.14)$$

Now, we will discuss the existing approaches to numerically characterize and discretize the viscosity solution approach. For references, we refer first to (Crandall and Lions, 1984), where monotone first-order approach is proposed. Later, in the work of (Osher and Sethian, 1988), higher order method was developed by utilizing the connections between conservation laws and Hamilton-Jacobi type PDEs. In this thesis, Godunov method, which is proposed in (Godunov, 1959), is used for the characterization of the motion in the normal direction. Despite the difficulties in implementing this method, it can properly characterize and satisfy the viscosity solution approach.

3.2.3 Numerical Discretization of the Front Evolution in the Normal Direction

In this thesis, we utilize the normal motion of the evolving front for representing the AUVs motion (assuming that there is no field force) from a given starting point on the $\phi(X, t = 0)$ to the any point on the $\phi(X, t = t_f)$. We utilize the Godunov method to characterize this front evolution in the normal direction.

The Godunov method is an exact numerical solution technique for the Riemann problem. Before we give the multi-dimensional formulation of Godunov method for Hamilton-Jacobi type equations, definitions are given. Let D^+ , D^- , and D^o be first order forward-difference, backward-difference, and the second order central-difference operators respectively. Therefore, the forward and the backward finite difference approximations for the differentiation of the signed distance function ϕ is given as

$$\frac{\partial\phi}{\partial x} \approx \frac{\phi_{i+1} - \phi_i}{\Delta x} \quad (3.15)$$

$$\frac{\partial\phi}{\partial x} \approx \frac{\phi_i - \phi_{i-1}}{\Delta x} \quad (3.16)$$

$$\frac{\partial\phi}{\partial x} \approx \frac{\phi_{i+1} - \phi_{i-1}}{2\Delta x} \quad (3.17)$$

Let I^x and I^y be intervals such that $I^x = [\phi_x^{min}, \phi_x^{max}]$ and $I^y = [\phi_y^{min}, \phi_y^{max}]$. Let also define $ext_x H$ and $ext_y H$ as follows. For all $\phi_x \in I^x$

$$ext_x H = \begin{cases} \min(H) & \text{if } D^- \phi_x < D^+ \phi_x \\ \max(H) & \text{if } D^+ \phi_x < D^- \phi_x \\ H & \text{otherwise} \end{cases}$$

Similarly, for all $\phi_y \in I^y$

$$ext_y H = \begin{cases} \min(H) & \text{if } D^- \phi_y < D^+ \phi_y \\ \max(H) & \text{if } D^+ \phi_y < D^- \phi_y \\ H & \text{otherwise} \end{cases}$$

By using the definitions above, the Multi-dimensional (in 2 dimensions) formulation of the Godunov scheme for Hamilton-Jacobi type equations can be written as

$$\hat{H} = ext_x ext_y H(\phi_x, \phi_y) \quad (3.18)$$

Basically, the statement made by Equation 3.18 can be described as follows. For the sake of brevity, we will consider one dimensional case. Assuming $V_n > 0$, H is minimized by $ext_x H$ if $D^- \phi_x$, $D^+ \phi_x$ are both positive and $D^- \phi_x < D^+ \phi_x$. H is maximized by $ext_x H$ if $D^- \phi_x$, $D^+ \phi_x$ are both positive and $D^- \phi_x > D^+ \phi_x$. Similarly, $ext_x H$ if $D^- \phi_x$, $D^+ \phi_x$ are both negative and $D^- \phi_x < D^+ \phi_x$. H is maximized by $ext_x H$ if $D^- \phi_x$, $D^+ \phi_x$ are both negative and $D^- \phi_x > D^+ \phi_x$. In the first case, we choose $D^- \phi_x$, and in the second case, we choose $D^+ \phi_x$, which are consistent with upwinding, Now, consider the case that a kink occurs, H is minimized by $ext_x H$ if $D^- \phi_x < 0$, $D^+ \phi_x > 0$, and $D^- \phi_x < D^+ \phi_x$. This minimization is achieved by setting $D\phi_x = 0$. H is maximized by $ext_x H$ if $D^- \phi_x > 0$, $D^+ \phi_x < 0$, and $D^- \phi_x > D^+ \phi_x$. This minimization is achieved by taking the maximum magnitude of $D^- \phi_x$ and $D^+ \phi_x$.

Even though the Godunov method is difficult to implement, because of its success to handle artificial dissipation and to characterize the viscosity solution of front evolution problem, it was chosen for this thesis work. In summary, It can be summarized as follows: for both positive or negative V_n

$$D\phi_x = \begin{cases} D^- \phi_x & \text{if } V_n D^- \phi_x > 0 \text{ and } V_n D^+ \phi_x > 0 \\ D^+ \phi_x & \text{if } V_n D^- \phi_x < 0 \text{ and } V_n D^+ \phi_x < 0 \\ 0 & \text{if } V_n D^- \phi_x \leq 0 \text{ and } V_n D^+ \phi_x \geq 0 \\ \max(|V_n D^- \phi_x|, |V_n D^+ \phi_x|) & \text{if } V_n D^- \phi_x \geq 0 \text{ and } V_n D^+ \phi_x \leq 0 \\ 0 & \text{otherwise} \end{cases} \quad (3.19)$$

In the paper "A Viscosity Solution to Shape from Shading", (Rouy and Tourin, 1992) proposed the scheme given in Equation 3.19 which elegantly characterizes the Godunov method.

$$D\phi_x^2 = \begin{cases} \max(\max(D^-\phi_x, 0)^2, \min(D^+\phi_x, 0)^2) & \text{if } V_n > 0 \\ \max(\min(D^-\phi_x, 0)^2, \max(D^+\phi_x, 0)^2) & \text{if } V_n < 0 \end{cases} \quad (3.20)$$

3.2.4 Front Evolution Due to Field Forces

In addition to our underwater vehicle speed which is characterized by front evolution in the normal direction, since underwater vehicles are subject to field forces such as ocean currents, the zero level set front evolution can be affected by externally generated velocity field $\vec{V} = \vec{V}(x, y, t)$. If there is no normal (vehicle in drift condition) motion but external velocity on the interface, the motion of the interface is same as external velocity field. For instance, if the velocity field on the interface is $\vec{V} = \langle 0, 1 \rangle$, and the $V_n = V_n(x, y) = 0$, then the interface is only driven by external velocity field and move up. We use the advection equation to simulate interface motion driven by an externally generated velocity field. The advected front evolution equation is

$$\phi_t + \vec{V}\nabla\phi = 0 \quad (3.21)$$

Even though the velocity field \vec{V} generally is defined on the whole domain Ω , it is better to use the field values in the band containing the zero level set of the signed distance function ϕ . One important advantage of band implementation is that less steep gradients may occur far from the zero level set $\phi = 0$ on the domain Ω . Therefore, we need less reinitialization of our signed distance domain. For more information, about reinitialization of the signed distance field, we refer to Subsection 3.2.8.

3.2.5 Numerical Discretization of the Front Evolution due to Field Forces

Let's consider the Godunov method discussed in subsection 3.2.3 again. In contrast to front motion in the normal direction, we have separate velocities u and v in every cartesian direction. Therefore, we can separate Equation 3.18 as follows

$$ext_x ext_y H = ext_x(u\phi_x) + ext_y(u\phi_y) \quad (3.22)$$

By using the Godunov method concept discussed in subsection 3.2.3, we can summarize the the approach used in this thesis as

$$D\phi_x = \begin{cases} D^- \phi_x & \text{if } u > 0 \\ D^+ \phi_x & \text{if } u < 0 \\ 0 & \text{if } u = 0 \end{cases} \quad (3.23)$$

$$D\phi_y = \begin{cases} D^- \phi_v & \text{if } v > 0 \\ D^+ \phi_v & \text{if } v < 0 \\ 0 & \text{if } v = 0 \end{cases} \quad (3.24)$$

Equations 3.23 and 3.24 are identical to standard Upwind Difference Method which was introduced by (Courant et al., 1952). On our domain, upwind difference method discretizes the signed distance domain by taking finite difference biased by the sign of characteristic speed of the front. By using the Equations 3.23 and 3.24, upwind difference scheme is summarized in Equation 3.25 and 3.26.

$$\begin{aligned} D\phi_x &= \max(u, 0)D^- \phi_x + \min(u, 0)D^+ \phi_x \\ D\phi_y &= \max(v, 0)D^- \phi_y + \min(v, 0)D^+ \phi_y \end{aligned} \quad (3.25)$$

3.2.6 Curvature-Driven Front Evolution

The last type of motion, which can be simulated by the level set method is curvature driven flow which is known as mean curvature driven motion of the interface. In the case of curvature driven motion of the interface, the interface moves in the normal direction with velocity proportional to its curvature. In the level set setting, the curvature dependent motion of the interface has only a component in the normal

direction. Therefore, the normal velocity can be defined as $\vec{V}_c = -b\kappa\vec{N}$ where b is a constant and κ is a curvature given in Equation 3.7. If $b < 0$, the interface moves in the direction of concavity. If $b > 0$, the interface moves to the direction of convexity. The curvature driven interface motion equation can be given as

$$\phi_t + V_c \nabla \phi = 0 \quad (3.26)$$

In this thesis work, we do not utilize the curvature-driven front evolution of the signed distance function. Therefore, we just content ourselves with a brief discussion of numerical characterization of the curvature-dependent signed distance function evolution. Since the second term of the Equation 3.26 is parabolic, central finite difference scheme is needed to characterize this equation (Malladi and Sethian, 1996), or the second order scheme that is used in (Agarwal and Lermusiaux, 2011) can be utilized. For the 2 dimensional case, the central difference scheme for the curvature-dependent motion can be written as

$$D\phi = b\kappa((D^o\phi_x)^2 + (D^o\phi_y)^2)^{\frac{1}{2}} \quad (3.27)$$

3.2.7 Putting Everything together

In order to obtain general interface evolution, we put equations 3.5, 3.21, and 3.26 together. Therefore,

$$\phi_t + \vec{V} \nabla \phi + V_n |\nabla \phi| - V_c \nabla \phi = 0 \quad (3.28)$$

In our path planning setting, we are not interested in curvature dependent term of the equation 3.28. Therefore, we are just interested in solving the first two terms of the equation 3.28. Therefore, the Equation 3.28 is reduced to Hamilton-Jacobi type PDE given in Equation 3.29, and the Equation 3.29 can be rewritten as in Equation 3.30.

$$\phi_t + \vec{V} \nabla \phi + V_n |\nabla \phi| = 0 \quad (3.29)$$

$$\phi_t + H(X, \vec{U}, \phi, \nabla \phi) = 0 \quad (3.30)$$

Now, we are beginning discussion of discretization of the Equation 3.30. Let H_1 and H_2 be $H_1 = u + V_n \phi_x |\nabla \phi|^{-1}$ and $H_2 = v + V_n \phi_y |\nabla \phi|^{-1}$ respectively. If the signs of u and V_n are same for both $D^- \phi_x$ and $D^+ \phi_x$, the front moves in the same direction with u and V_n . Therefore, by referring the Equations 3.19 and 3.23, we set $D\phi_x = D^- \phi_x$.

Now, consider the case where u and V_n do not have same sign. This means that the normal motion and advected motion of the front are in opposite directions. In order to satisfy upwinding requirements, one needs to determine the dominant motion of the front. Therefore, by referring to the Equation 3.19 and 3.23, we can make our characterization of the front evolution in 2 dimension, as follows:

$$D\phi_x = \begin{cases} D^- \phi_x & \text{if } H_1 > 0 \text{ for both } D^- \phi_x \text{ and } D^+ \phi_x \\ D^+ \phi_x & \text{if } H_1 < 0 \text{ for both } D^- \phi_x \text{ and } D^+ \phi_x \\ \max(|D^- \phi_x|, |D^+ \phi_x|) & \text{if } H_1 > 0 \text{ for } D^- \phi_x \text{ and } H_1 < 0 \text{ for } D^+ \phi_x \\ \frac{-u}{V_n} & \text{if } H_1 < 0 \text{ for } D^- \phi_x \text{ and } H_1 > 0 \text{ for } D^+ \phi_x \\ 0 & \text{otherwise} \end{cases} \quad (3.31)$$

$$D\phi_y = \begin{cases} D^- \phi_y & \text{if } H_2 > 0 \text{ for both } D^- \phi_y \text{ and } D^+ \phi_y \\ D^+ \phi_y & \text{if } H_2 < 0 \text{ for both } D^- \phi_y \text{ and } D^+ \phi_y \\ \max(|D^- \phi_y|, |D^+ \phi_y|) & \text{if } H_2 > 0 \text{ for } D^- \phi_y \text{ and } H_2 < 0 \text{ for } D^+ \phi_y \\ \frac{-v}{V_n} & \text{if } H_2 < 0 \text{ for } D^- \phi_y \text{ and } H_2 > 0 \text{ for } D^+ \phi_y \\ 0 & \text{otherwise} \end{cases} \quad (3.32)$$

Note that if $H_1 < 0$ for $D^-\phi_x$ and $H_1 > 0$ for $D^+\phi_x$, we set $D\phi_x$ is equal to $-u/V_n$ because the Godunov method chooses the minimum value for H , and this relative minimum occurs when H_1 is equal to zero. This statement is also valid for H_2 .

In this thesis work, the method Godunov method is utilized to characterize the front evolution. We define the front zero level set of the signed distance function ϕ . Despite the success of Godunov method to characterize the front evolution, as the front evolves, the signed distance function field generally loses its signed distance property. In the next subsection, we will discuss this issue of the signed distance function.

3.2.8 Construction and Reinitialization of the Signed Distance Field

As it is stated in the previous subsection, the signed distance function needs to be initialized to start calculations and reinitialized during the run to avoid numerical instabilities. In seminal work of (Osher and Sethian, 1988), the signed distance function is initialized by using $\phi = 1 \mp d^2$ where the distance function d takes the minus sign in Ω^- and positive sign in Ω^+ . In the work of (Mulder et al., 1992), it is shown that $\phi = \mp d$ is a better choice which gives better results than approach of (Mulder et al., 1992).

In the work of (Chopp, 1993), the notion of reinitialization is introduced. In this work, reinitialization is realized by stopping calculations at certain frequency and by calculating distance of every point on the domain Ω from the zero level set contour $\phi = 0$. In this thesis work, reinitializations for 3 dimensional calculations is of this type. In order to discretize and locate the zero level set of the function ϕ during the 3 dimensional calculations, we utilize crossing time approach proposed for the image processing applications in the series of papers (Bruckstein, 1988), (Kimmel and Bruckstein, 1992), and (Kimmel and Bruckstein, 1993).

In order to find the zero level set front of the signed distance function ϕ , we find isocontours of the crossing times. We utilize interpolation techniques to find the crossing time isocontours if the zero level set front does not lie on the grid points. Assume that we stop calculations at time T . This time T contour gives the zero level set of the signed distance function ϕ . Then, we calculate distance every point on the domain from time T isocontour. If the grid point crossing time t_{grid} is less than T , the distance takes negative sign. If the grid point crossing time (predefined) t_{grid} is greater than T , the distance takes positive sign. Therefore, we can re-construct our signed distance field again.

For the 2 dimensional calculations, instead of calculating every grid point distance from the zero level set contour, we utilize fast marching approach which can accurately calculate the signed distance field. More information regarding reinitialization with the fast marching approach will be given in Section 3.3. Several reinitialization approaches have been proposed to avoid numerical losses on the signed distance field. For more information and recent advances about reinitialization of the level set calculations, we refer the reader interested in reinitialization of the signed distance field to (Russo and Smereka, 2000), (Sussman et al., 1994), and (Sussman and Fatemi, 1999).

3.3 Fast Marching Method

3.3.1 Introduction

Before introducing fast marching method, we should first consider Dijkstra algorithm. The Dijkstra algorithm is closely related to the fast marching method. It can be said that the fast marching method is a continuous formulation of the Dijkstra algorithm (Sethian, 2001). Dijkstra's algorithm, first introduced by Edsger Dijkstra in 1956 (Dijkstra, 1959), is a graph search algorithm that finds the shortest path between given start and terminal points on the graph. This algorithm is widely used in robotics, computer science, and several engineering disciplines.

3.3.2 Dijkstra Algorithm

Now, let us give the definition of the Dijkstra shortest path algorithm. Given weighted graph $G(V, E)$, the shortest path between any 2 vertex on this graph can be found by the algorithm given below.

1. At the beginning all nodes are marked as unvisited. Set start node as current node
2. Compute temporary distance from current node to all neighbor nodes. For example, if the recorded distance from any neighbor node to initial node is less than the previously recorded distance from initial node to this neighbor node, overwrite the previously recorded distance to this neighbor node. When we are done with checking all neighbors of the current node, mark the current node as visited. A visited node will never be visited again, and the recorded distance of visited node is eventual and optimum.
3. If all the nodes have been marked as visited, finish the process. Otherwise, continue with the smallest distance as the next "current node" and continue from step-2.

The complexity of the Dijkstra's Algorithm is $O(M \log M)$. The Dijkstras Algorithm gives the solution to the discrete optimal path planning problem on a given cartesian grid. Mathematically, the Dijkstra's Algorithm can be stated as follows (Sethian and Vladimirsky, 2004); consider a cartesian grid domain with grid size Δh . The cost for crossing each grid point $X_{ij} = (i\Delta h, j\Delta h)$ in this domain is given as $J_{ij} > 0$. Therefore, the optimum cost function for the neighbor point of X_{ij} , for instance, for the point $X_{i+1,j}$ can be found as follows

$$J(X_{i+1,j}) = \min(f(X_{i,j})c(X_{i+1,j}) + J(X_{i,j})) \quad (3.33)$$

where f is weight associated with the point $X_{i,j}$, c is cost to go from $X_{i,j}$ to $X_{i+1,j}$, and $J(X_{i,j})$ is minimum accumulated cost at the point $X_{i,j}$.

3.3.3 Fast Marching Algorithm

Fast marching algorithm is a numerical method to solve the nonlinear Eikonal equation. On the rectilinear grid domain which has M grid points, analogously, the complexity of the fast marching algorithm is $O(M \log M)$ (Sethian, 2001). Dijkstra-like continuous viscosity solution formulation approach for solving the Eikonal equation is proposed in the seminal papers of (Tsitsiklis, 1994) and (Tsitsiklis, 1995). Then, in the paper of (Sethian, 1996a), the upwind difference method is proposed to characterize viscosity solution approach proposed in (Tsitsiklis, 1995) and fast marching idea is shown. For more information, we refer to (Sethian and Vladimirsky, 2004).

It can be said that fast marching is a stationary and continuous formulation of the front evolution characterized by Eikonal Equation. See Equation 2.1. The term τ in the Equation 2.5 can be considered as the term $f(X)c(X)$ in the equation 3.33. As in Dijkstra algorithm, the upwind difference operator with signed distance function ϕ decides which grid point to update first (Step-2 of Dijkstra Algorithm) by solving the Eikonal Equation. This continuous update is realized by the viscosity solution which is characterized by the upwind difference method. For the two dimensional case, the upwind difference method used for the fast marching algorithm is given in Equation 3.34 (Sethian and Vladimirsky, 2000). Note that the μ becomes $\mu = T$ in this case.

$$\left[\begin{array}{l} \max(D^-T_x, -D^+T_x, 0) \\ \max(D^-T_y, -D^+T_y, 0) \end{array} \right] = \tau \quad (3.34)$$

The algorithm for the fast marching method can be stated as follows

1. Mark all the neighbor points which are lies on and inside initial front as accepted, and mark all the other points in the domain as considered. See Figure 3-3.
2. Mark all the points close to the front as trial. If the points in the trial set are

far from the front remove them and put them back to the set of considered, form a narrow band as in the Figure 3-3.

3. Mark trial points to set of accepted points.
4. Recalculate the values of T at all neighbors of Trial points by using Equation 3.34.
5. Return to second step of the algorithm.

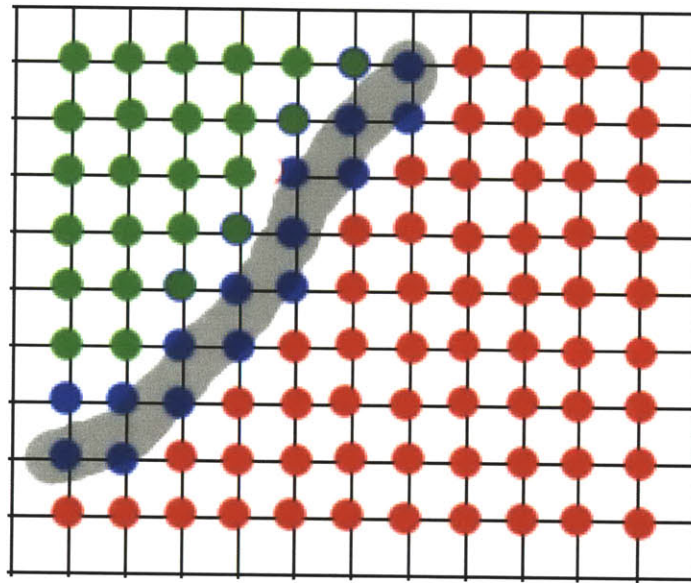


Figure 3-3: Fast Marching Algorithm; red points represents set of accepted points, blue Points represents set of trial points

Fast marching algorithm has been used in many different areas such as geosciences (Agarwal and Lermusiaux, 2011), medical imaging (Parker et al., 2002), etc. It is faster than level set method, and implementation is not complicated. One drawback of the fast marching algorithm is that it can only be used for fronts evolving in the outward or inward, but not in the both direction. However, for the purpose of reconstructing signed distance field, fast marching method is the accurate way of doing it. Therefore, we utilize it for the reinitialization of the signed distance field of the two dimensional path planning calculations.

3.3.4 Reinitialization of the Signed Distance Field with Fast Marching

Unfortunately, the signed distance function loses its signed distance property after a certain time step. The frequency of reinitialization depends on calculation and are determined by experience. The idea of reinitialization with fast marching algorithm is stated as follows.

- At certain time steps, stop level set calculations
- Solve the Equation 3.35 and evolve front in the outward direction, using points that lie on the zero level set $\phi = 0$ as the initial accepted points. Note that interpolation is needed if the zero level set does not lie on the grid points.

$$|\nabla\phi_{ini}| = 1 \tag{3.35}$$

- Solve the Equation 3.35 and evolve front in the inward direction, using points that lie on the zero level set $\phi = 0$ as the initial accepted points. Again, interpolation is needed if the zero level set does not lie on the grid points.
- Set $\phi = \phi_{ini}$
- Continue level set calculations.

3.4 Backward Calculations

In this section, since one of the steps of our path planning algorithm includes backwards computation for finding contour normal curves, We will discuss solution method we used in this thesis. Along the level set calculations, we record history of level set motion by recording crossing times. Therefore, at the end of the calculations we have crossing time contours characterized by T_{cross} . This is a major new contribution of this work. Examples of crossing time contours are given in Chapter 4 Section 4.3.

In order to find normal to these contours, we solve the following ordinary differential equation (ODEs).

$$X_t = \nabla T_{cross} \tag{3.36}$$

There are many different approach for integration of ODEs, such as the Runge-Kutta method, Leapfrog integration for initial value problems, and collocation methods for boundary value problems (Hoffman, 2001). In this thesis work, we utilize the Euler method to solve the Equation 3.36. The mathematical description of the Euler method is given as follows (Ascher and Petzold, 1998). Given $h' = F(h(t), t)$ and $h(t_0) = h_0$, the equation for Euler method

$$h_{n+1} = h_n + \Delta t F(h(t_n), t_n) \tag{3.37}$$

where Δt is time step. Note that the Equation 3.37 shows the forward solution, but in our algorithm, we solve it backwards in time.

In this chapter, we have discussed all the necessary mathematical background to produce our path planning solution. In the next chapter, we will begin presenting our algorithm based on the information given in this chapter.

Chapter 4

Underwater Path Planning

4.1 Introduction

The aim of this chapter is to present the path planning algorithm based on the theory given in Chapter 3 and its applications in computer. An advantage of this algorithm is that there is no special implementation needed to handle strong or complicated ocean currents. The path planning algorithm presented here can easily find feasible trajectories in the presence of strong currents. It can easily characterize non-linear response of AUVs to complicated ocean flows.

Another advantage of our algorithm is its tractability even for multi-agent based settings. In case of AUVs deployment from different locations, the cost of the algorithm increases linearly, and in case of same location deployment of AUVs, the cost is just increased by the cost of backward calculation step of the algorithm. See Section 4.2 for backward calculation.

In this section first, we will present algorithm for the path planning. Then we present the applications as test cases to demonstrate the abilities of our algorithm.

4.2 Algorithm

The basic idea of the algorithm is to represent vehicle motion by evolving a front which is characterized by $\phi = 0$. One of the important differences of our path planning algorithm is backward calculations for producing feasible and optimal trajectories. In order to find feasible trajectories, we subtract the corresponding velocity from trajectory given by crossing time contours. The idea of subtracting velocities from the trajectory, which is normal to the crossing time contours, is introduced by Mattheus Ueckermann (M.S) during the discussion of the path planning problem. The path planning algorithm for AUVs, which is the core of this thesis work, can be stated as follows

1. Initialize the signed distance domain $\phi \in \Omega$ as in stated in Subsection 3.2.8. and set the vehicle speed V_n . Note that the start point of our vehicle takes the value of $\phi = 0$. If we work with ocean prediction system, proper scaling of the domain Ω must be done.
2. Solve Equation 3.30 for determined time step Δt by utilizing Equations 3.20 and 3.25 with considering Equations 3.31 and 3.32.
3. Record crossing time T of each point on the domain Ω . Return to step-2 or at every certain frequencies of the calculation time, stop calculations and go to step-4. If the goal point is in the Ω^- , go to step-5.
4. Re-construct the signed distance field ϕ . For the 2 dimensional case, use Equation 3.35, considering the information given in Subsection 3.3.4. For the 3 dimensional case re-construct the signed distance field as it is stated in Subsection 3.2.8. Return to step-2 of the algorithm.
5. Adapt Equation 3.37 to our domain and solve it backwards in time and subtract corresponding velocity. Continue until reaching start point.

4.3 Applications and Test-Cases

Test-Case1: In Test-Case 1, our AUV is deployed from $x = 0, y = 0$ and the goal point is at $x = 0.8, y = 0.8$. The speed of AUV is 1 m/s, The speed jet flow, which is shown as a narrow band with black arrows, is constant $u=0.5$ and in the direction of $+x$. As it can be seen from Figure 4-1, AUV changes its trajectory angle when it reaches flow field and takes the advantage of the flow field to optimally reach goal point.

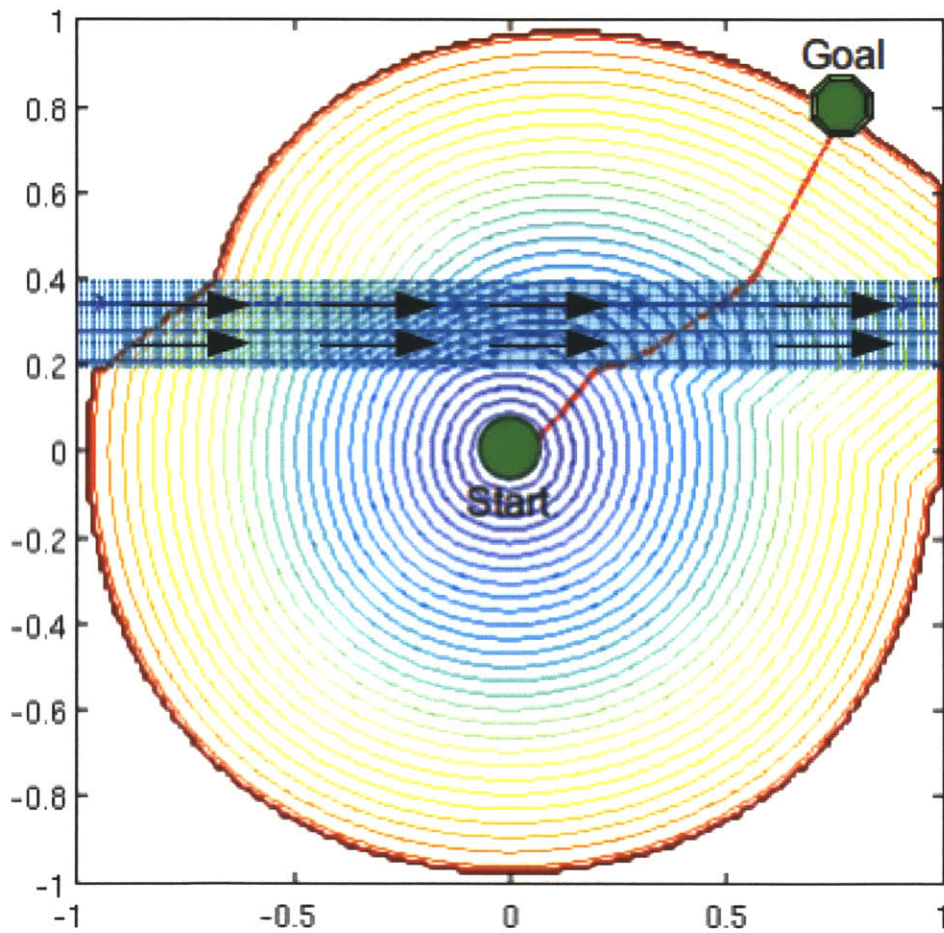


Figure 4-1: Test-Case 1

Test-Case2: In Test-Case 2, our AUV is deployed from $x = 0, y = -0.3$ and the goal point is at $x = -0.75, y = 0.75$. The speed of AUV is 1 m/s, In contrast to the

Test-Case 1. The speed of jet flow, which is shown as narrow band with black arrows, is higher than AUV speed and constant $u=0.5$ m/s, and it is in the direction of $+x$. As it can be seen from Figure 4-2, AUV can find the feasible trajectory and take advantage of the flow field even its speed is higher than AUV speed.

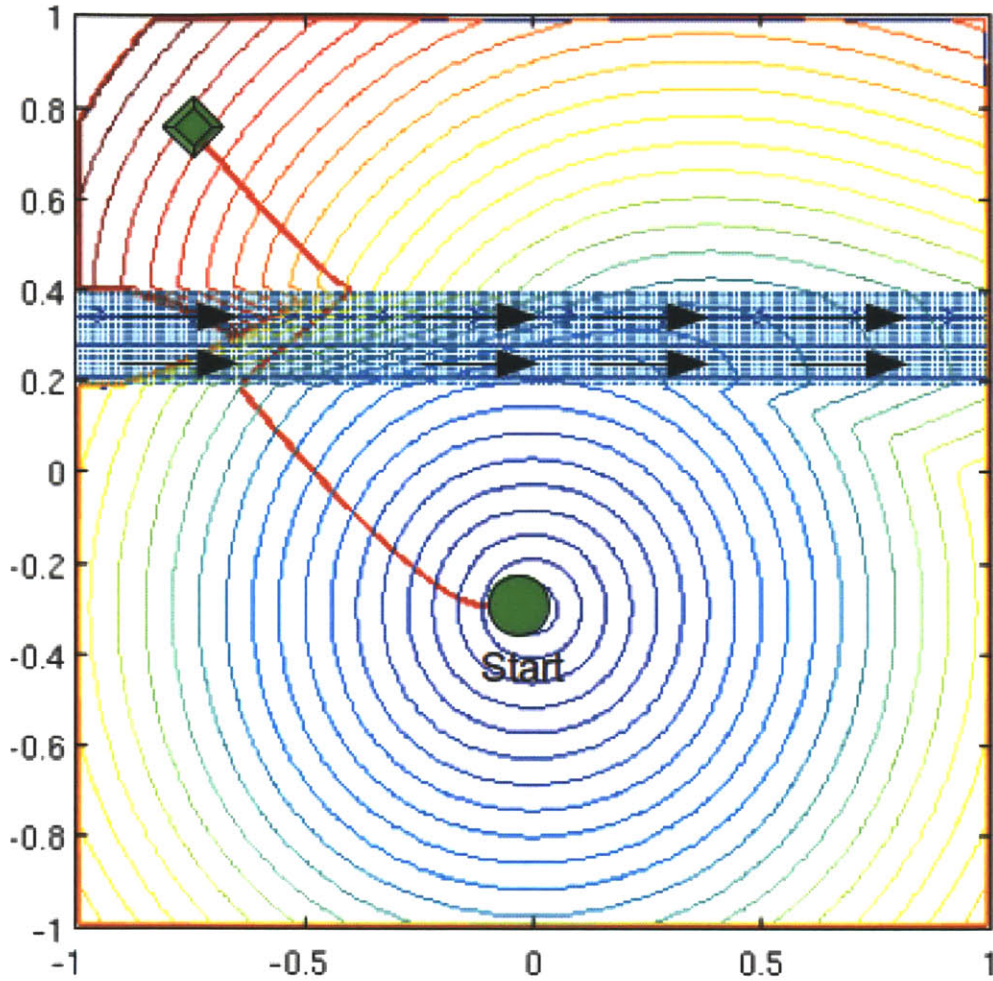


Figure 4-2: Test-Case 2

Test-Case3: In Test-Case 3, our AUV is deployed from $x = 0, y = -0.4$ and the goal point is at $x = 0, y = 0.8$. The speed of AUV is 1 m/s, In this case, we have two different jet flow. The first jet flow, which is shown as narrow band with black arrows on the left, has a speed higher than AUV speed and constant $v_1 = 2$ m/s, and

it is in the direction of $+y$. The second jet flow, which is shown as narrow band with red arrows on the right, has a speed equal to AUV speed and constant $v_2 = 1m/s$, and it is in the direction of $+y$. As it can be seen from Figure 4-3, AUV takes the advantage of the higher jet flow on the right to optimally reach the goal point.

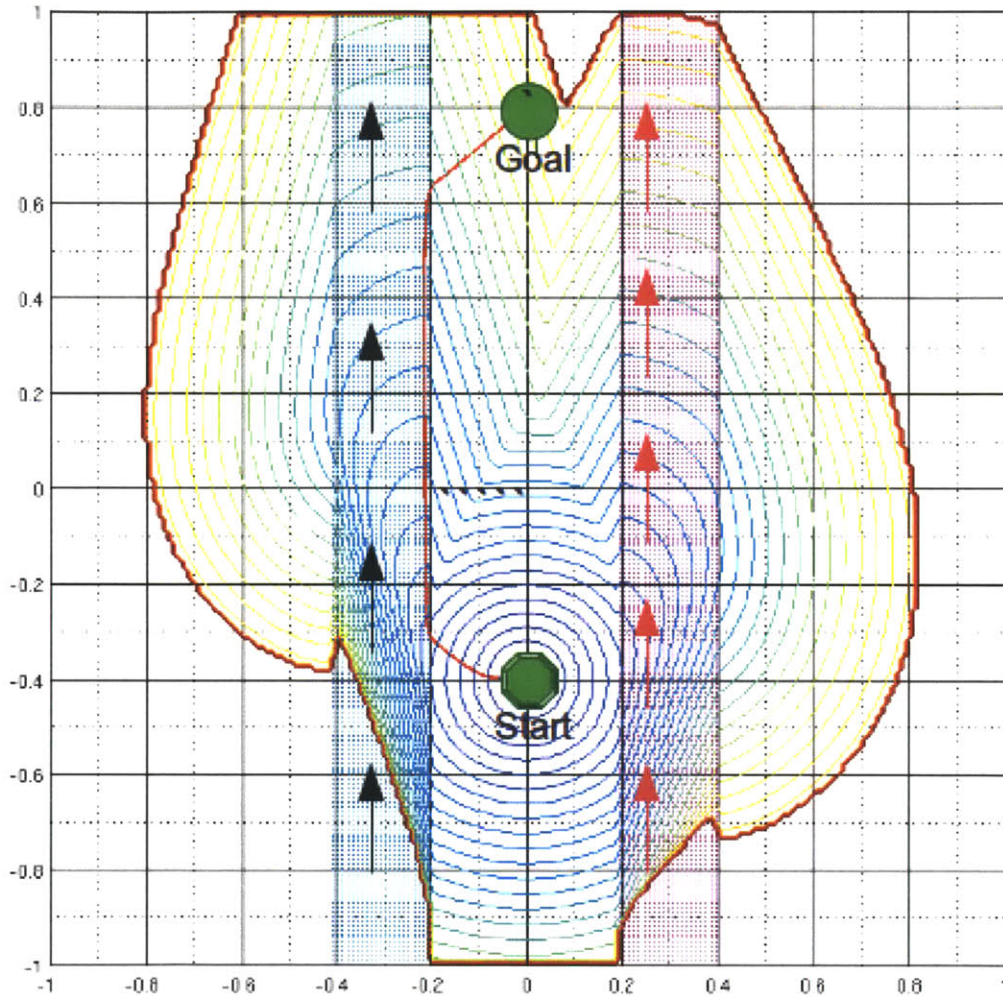


Figure 4-3: Test-Case 3

Test-Case4: In Test-Case 4, our AUV is deployed from $x = -0.6, y = -0.6$ and the goal point is at $x = 0.6, y = 0.6$. The speed of AUV is 1 m/s, In this case, we have two different jet flowing in the inverse directions. The first jet flow, which is shown as narrow band above with black arrows, has a speed higher than AUV speed and

constant $u_1 = 1.5m/s$, and it is in the direction of $-x$. The second jet flow, which is shown as narrow band below with red arrows, has a speed higher than AUV speed and constant $u_2 = 1.5m/s$, and it is in the direction of $+x$. As it can be seen from Figure 4-4, the AUV first finds feasible trajectory to cross jet flow below and takes the advantage of this flow. Then, in order to optimally reach goal point, AUV takes the advantage of the jet flow above.

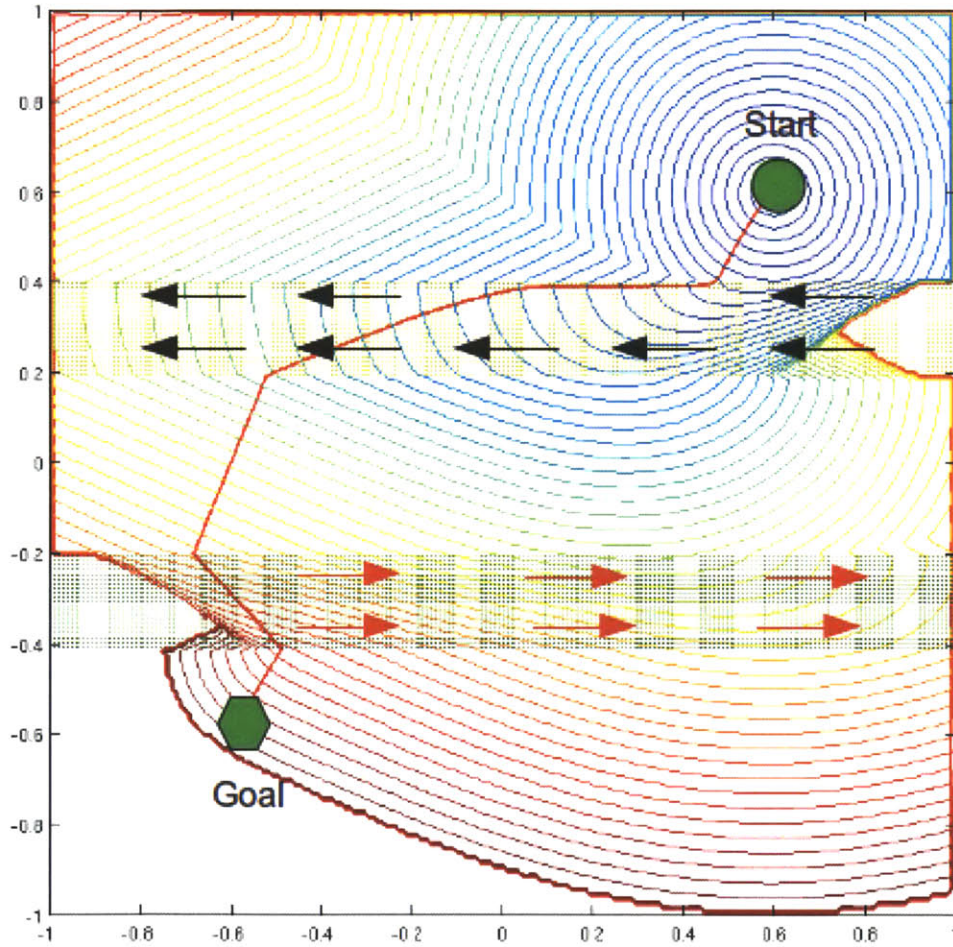


Figure 4-4: Test-Case 4

Test-Case5: In Test-Case 3, our AUV is deployed from $x = -0.6, y = 0.6$ and the goal point is at $x = -0.6, y = -0.6$. The speed of AUV is 1 m/s, In this case, we have two different jet flow. The first jet flow, which is shown as narrow band above with red arrows, has a speed higher than AUV speed and constant $v_1 = 1.5m/s$, and

it is in the direction of $+y$. Therefore, it is infeasible to use any trajectory crossing jet flow above. The second jet flow, which is shown as narrow band below with black arrows, has a speed higher than AUV speed and constant $u_2 = 1.5m/s$, and it is in the direction of $+x$. As it can be seen from Figure 4-5, AUV first finds the optimal trajectory, which is to flow on the right side of the narrow band above, then to cross the jet flow below. Then, In order to optimally reach goal point, AUV takes the advantage of the jet flow below.

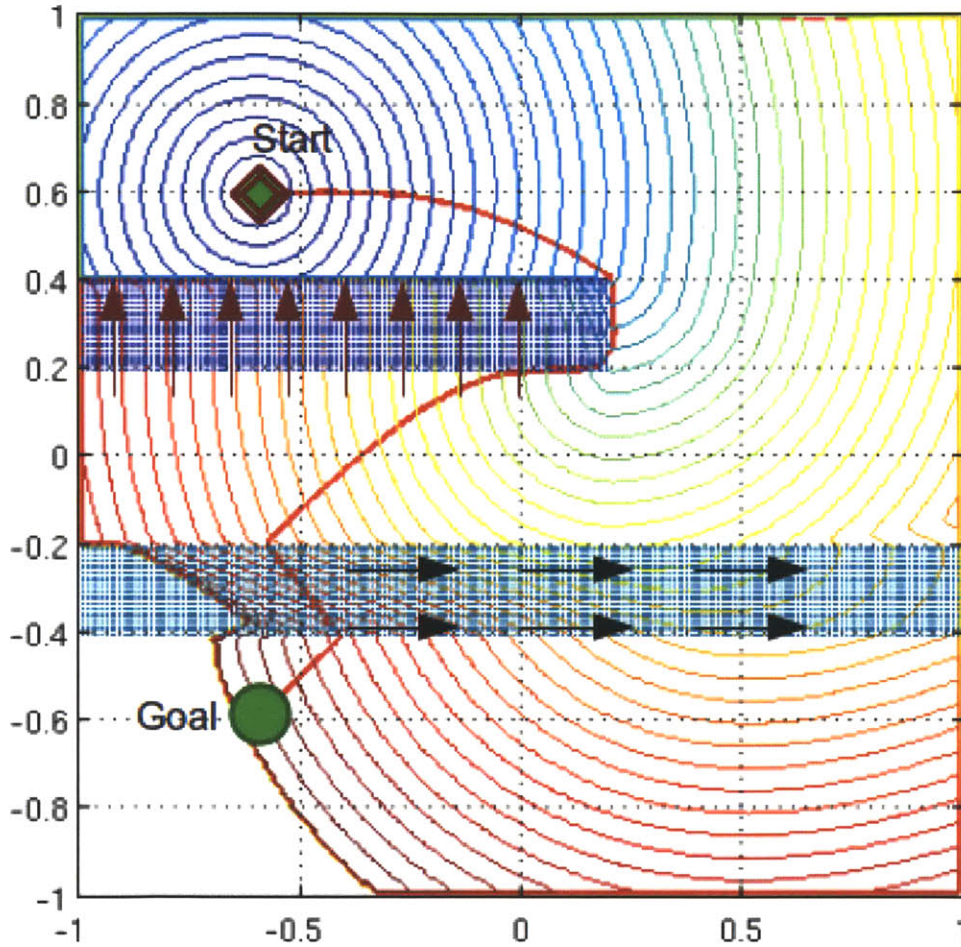


Figure 4-5: Test-Case 5

Test Case 6 In this test-case, we are interested in path planning in the presence of complicated flows. lid-driven Cavity flow was chosen to simulate complicated flow fields. The lid-driven cavity flow is a standard test or validation flow to test new

developed codes (Botella and Peyret, 1998). The lid-driven flow domain has simple 2 dimensional geometry. In this thesis work, we utilized the standard case where flow field is restricted in a square domain. Dirichlet conditions are applied to three stationary boundary and one moving boundary. See Figure 4-6. The resultant flow with the zero level set of ϕ , which is shown as turquoise curve, can be seen in Figure 4-7.

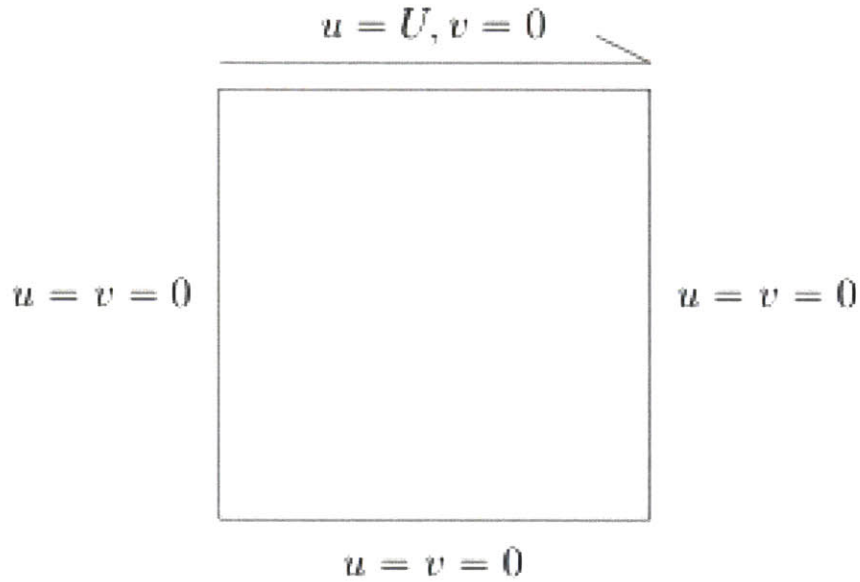


Figure 4-6: Boundaries of Lid-Driven Cavity Flow Domain

In Test-Case 6, our AUV is deployed from $x = 0.5, y = 0.5$ and the goal point is at $x = 0.8, y = 0.5$. The speed of AUV is 0.4 m/s. The maximum speed is realized during the simulation time in the flow domain is 0.6 m/s, which is higher than AUV speed. As it can be seen from Figure 4-8, AUV first finds the optimal trajectory to reach the goal point

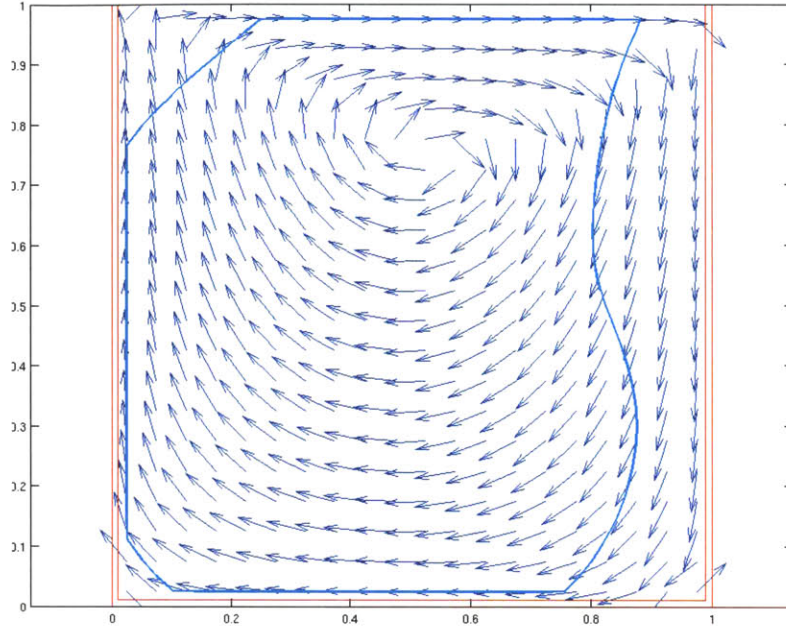


Figure 4-7: Time Dependent Lid-Driven Cavity Flow with front evolution

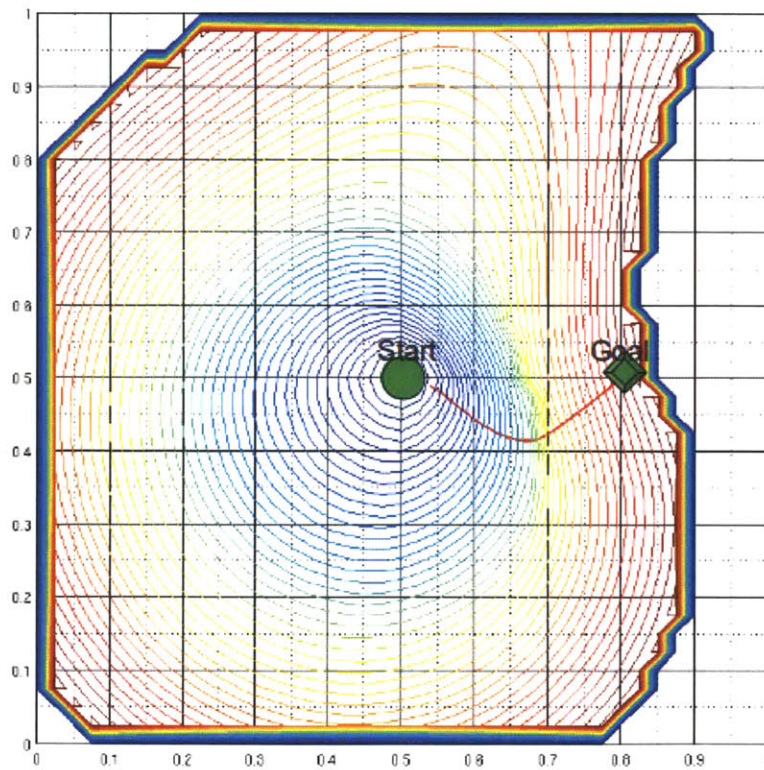


Figure 4-8: Test-Case 6

Test-Case 7 In Test-Case 7, we show how the AUV can take advantage of the complicated flow fields by using our path planning algorithm. The flow data used in this case is same as Test-Case 6. In this case, our AUV is deployed from $x = 0.5, y = 0.3$ and the goal point is at $x = 0.5, y = 0.9$. The speed of AUV is 0.4 m/s. The maximum speed realized along the simulation time in the flow domain is 0.6 m/s, which is higher than AUV speed. As it can be seen from Figure 4-9, instead of moving in straight route to goal point, our AUV follows curve trajectory which provides feasible trajectory and advantage of the lid-driven cavity flow field.

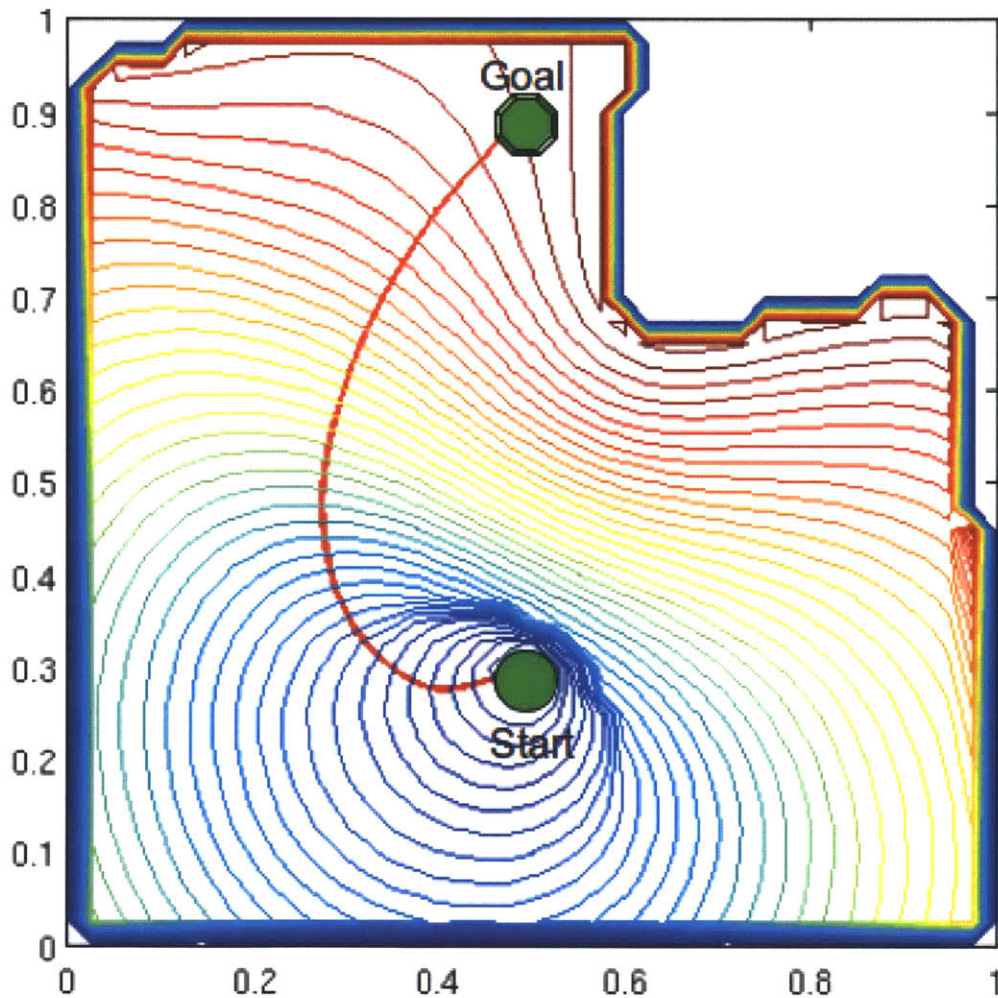


Figure 4-9: Test-Case 7

4.4 Path Planning with Ocean Prediction System

In this section, we show the path planning application combined with Ocean prediction system. In our framework, the MSEAS ocean prediction system is used as data provider for our path planning algorithm. The ocean prediction data is taken from realistic ocean predictions based on the real-time AWACS and SW06 exercises (Aug.Sep. 2006) in the New Jersey Shelf/Hudson Canyon region (Lermusiaux, 2006) (Haley and Lermusiaux, 2010). The domain is a 172 155-km domain, with 1-km resolution and 30 vertical levels. Objective analyses were used for estimation of the initial conditions, using the data gathered by gliders, AUVs, ship deployed conductivity temperature depth (CTD) and the historical data taken from World Ocean Database, Gulf Stream Feature analyses, National Marine Fisheries Service, etc. The duration for this real-time ocean prediction simulation was 43.5 days. Here, we focus on the period during which Tropical Storm Ernesto passes by the region in late August - early September, 2006.

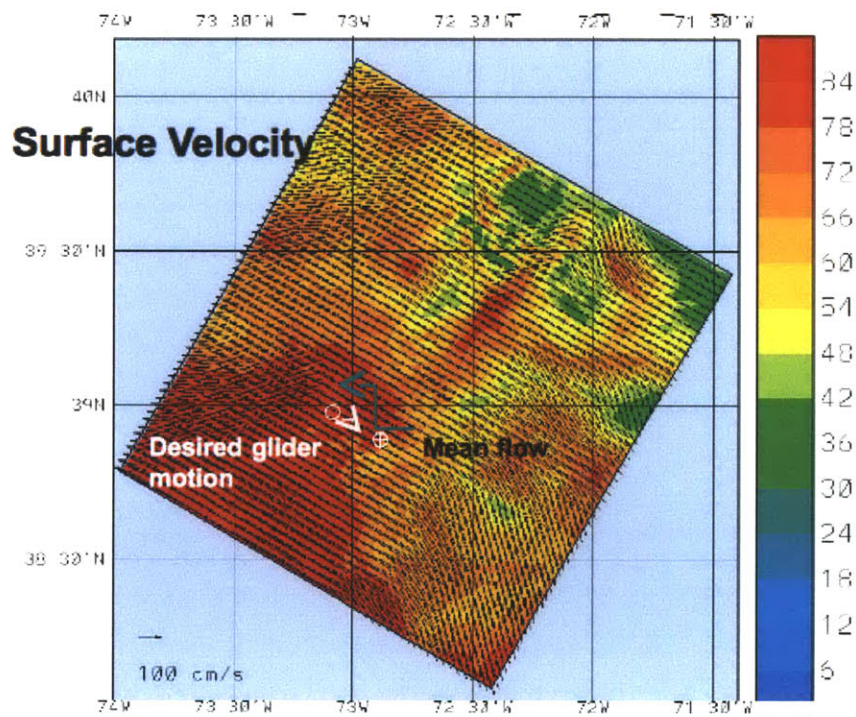


Figure 4-10: Ocean Flow Prediction on Near Surface level

In order to simulate realistic and most practical conditions, we set our vehicle speed to 0.25 m/s, which is most of the currently operated underwater gliders' maximum speed. The goal of vehicle is to reach the goal location from start position which are shown in Figure 4-10. In this simulation, we use ocean prediction data of Middle Atlantic Bight region, which is subject to tropical storm Ernesto. Therefore, if the glider use the straightforward trajectory from start location to goal location, it is impossible to reach goal location because of the strong ocean currents in the region. However, by using the algorithm presented in this thesis in 3D, our glider dive into deep, near bottom levels (80 m) of the ocean, and it takes the advantage of the flow field in the deep ocean region. See Figure 4-11 for the near bottom flow field. Note that the colormap shown in Figures 4-10 and 4-11 are velocities(m/s) of ocean currents.

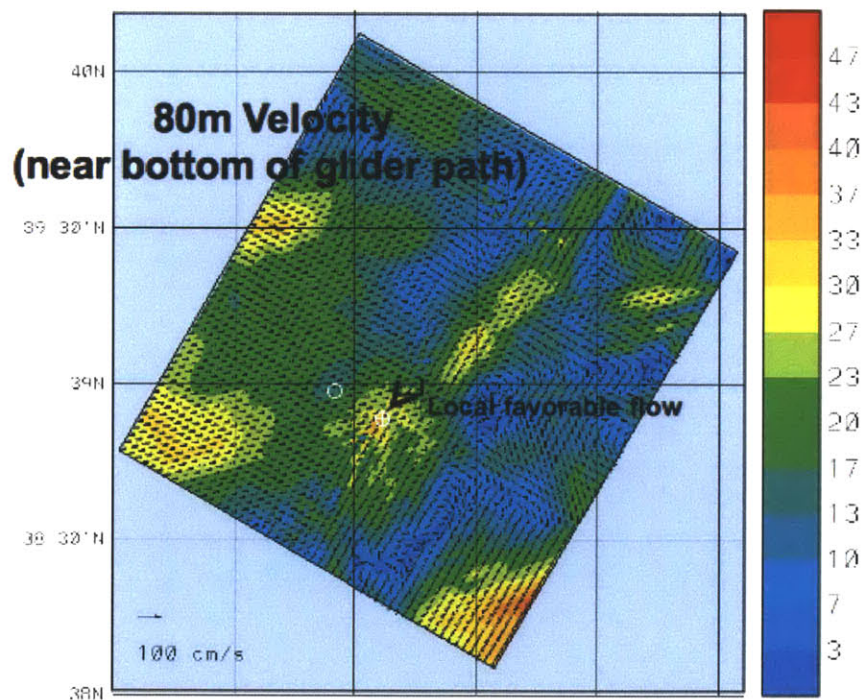


Figure 4-11: Ocean Flow Prediction on Near Bottom level

In this chapter, we have presented our new 3D path planning algorithm for AUVs. As it is shown in Section 4.4, our path planning algorithm can be used in real-time

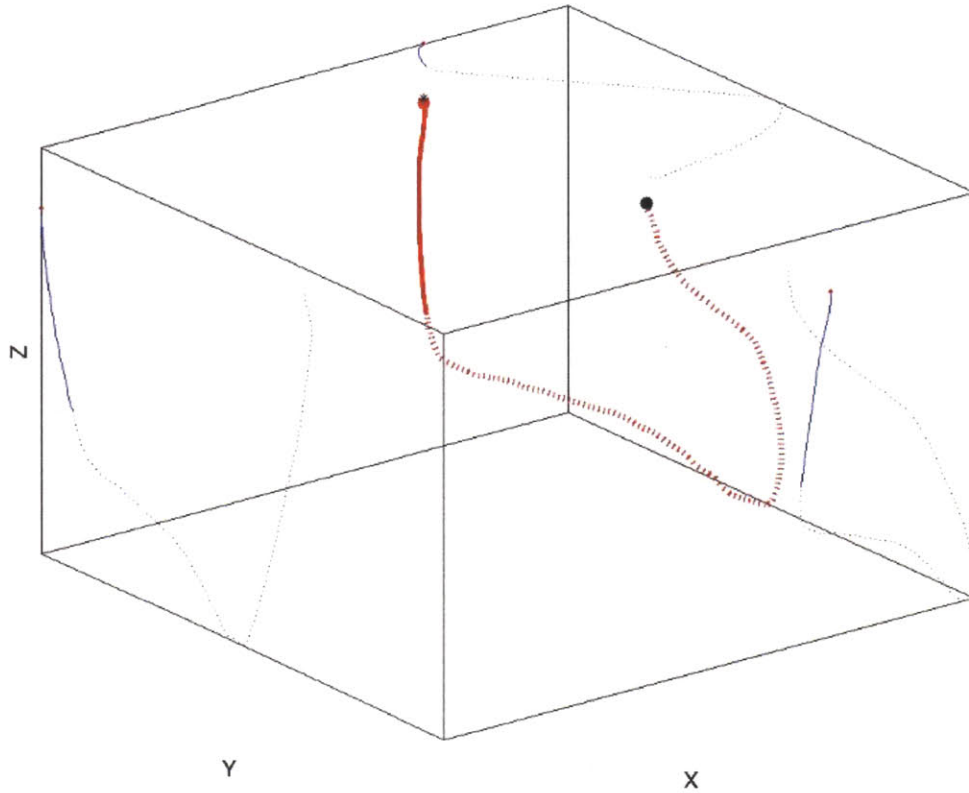


Figure 4-12: 3D Path Planning, red curve represents 3D Trajectory and other curves represent projections on cartesian planes

operations carried out by underwater gliders and vehicles. On the other hand, the capabilities of our path planning algorithm is not limited to underwater path planning. It can also be used for autonomous sea surface vehicles, vehicles operated in the atmosphere such as montgolfier balloons, or any environment that has a dynamic flow. Other possible improvements for our path planning algorithm are discussed in the next chapter.

Chapter 5

Conclusions

From the naval operations to the scientific missions, the importance of autonomous vehicles is increasing with the advancing underwater robotics technology. There is no doubt that one crucial part of these autonomous underwater missions is to produce optimal and feasible paths. The goal of this thesis is to propose an optimal, feasible, and tractable underwater path planning algorithm which can be utilized for autonomous underwater vehicle operations. In order to fulfill this goal, a comprehensive review of existing underwater path planning and related robotics path planning algorithms together with the advantages and disadvantages of these methods were discussed in Chapter 2. Then, the underpinning theory of the presented underwater path planning algorithm, which is level set method, was discussed in Chapter 3. Detailed discussion of numerical and theoretical aspects of the level set method was made. In Chapter 4, our path planning algorithm was presented. In order to show the capabilities of presented algorithm, many realistic and non-realistic test cases are demonstrated. Finally, to show the real-time capabilities of our algorithm, 3D path planning together with the Multidisciplinary Simulation Estimation and Assimilation System (MSEAS) data was demonstrated.

We believe that level set method is a promising framework to produce optimal, feasible, and practical solutions for underwater path planning, and the presented path

planning algorithm can be developed and extended in many ways. The summary of the results and the future work suggestions are stated as follows.

5.1 Summary of Results

One of the advantage of the presented algorithm is its capability and efficiency to handle non-linear response of the underwater vehicles to complicated time-dependent and intermittent ocean flows. It was demonstrated that even in fully chaotic flow environment, our algorithm can work without any need of special implementation.

Second, in addition to built-in capability of handling complicated flows, our path planning algorithm can easily produce feasible trajectories without need of special implementation. If the algorithm cannot produce any feasible trajectory between start and goal points, that means there is no feasible trajectory in the problem domain.

Third, since the ocean has complicated dynamics and analytically unpredictable behaviors, ocean prediction and simulation models, such as MSEAS, must be used in order to produce reasonable predictions of optimal paths.. The presented algorithm can easily work with ocean prediction system with just making minor modifications, such as scaling and smoothing of the fronts. This was completed for an example in the Middle Atlantic Bight region in ocean conditions corresponding to the passage of a tropical storm.

Fourth, a very important aspect of our algorithm is that its tractability and accuracy even for large ocean domains and data.

Finally, in case of multi-vehicle operations, if the vehicles are deployed from same location, the cost of our algorithm is just increased by the cost of the backwards solution needed for each vehicle. The level set framework is open to improvements, and many modification can be made to improve the presented algorithm. On the

other hand, many exciting research questions are waiting to be explored. In the next subsection, we will discuss these open research questions and suggestions.

5.2 Suggestions and Future Work

One important constraint of real-time underwater vehicle operations is that computational cost of path planning algorithms. For our path planning algorithm, the computational cost can be decreased by implementing well-defined level set solutions, such as narrow band level set method (Adalsteinsson and Sethian, 1995), sparse field level set method (Whitaker, 1998), sparse block grid level set method (Bridson, 2003), octree level set method (Strain, 1999) and (Losasso et al., 2004), run-length encoded level set method (Houston et al., 2006) and (Nielsen and Museth, 2006), and for non-uniform ocean data, point based level set method (Corbett, 2005). For instance, one improvement can be made by implementing narrow band level set method. In the narrow band implementation of the level set method, since the calculations are carried out in the small band around the zero level set, the computational cost decreases considerably.

Considerable amount of computational cost of our path planning algorithm comes from the reinitialization of the signed distance domain. Instead of implemented reinitialization approaches used for this thesis work, more efficient reinitialization schemes can be used for decreasing the computational cost of our path planning algorithm, such as method proposed in (Sussman et al., 1994). On the other hand, determining the frequency of reinitialization during the path planning calculations is still open research question. There is no doubt that if ideal forms of reinitialization are determined, this will lead to more efficient autonomous underwater vehicle operations.

Another open research question is to develop fully consistent level set numerical scheme to combine path planning algorithm with the ocean prediction system. In addition to that, combining stochastic ocean predictions with our path planning schemes

remains as exciting research subject. Currently, The Multidisciplinary Simulation Estimation and Assimilation System Group of MIT is exploring this promising research question.

Appendix A

Description of Matlab Files

A.1 Matlab Scripts for Two Dimensional Calculations

cavitypathplanning.m (Function) : This matlab function conducts path planning in the presence of cavity flow. It uses cavity flow data supplied by the user. It can also be used for other data without need of special implementation. Note that data must be in the search directory of Matlab. The structure of cavitypathplanning.m function is stated as follows.

```
cavitypathplanning.m(rx0,ry0,rx,ry)
```

where $rx0$ is cartesian x coordinate of start point, $ry0$ is cartesian y coordinate of start point, rx is cartesian x coordinate of goal point, and ry is cartesian y coordinate of goal point.

pathplanning2d.m (Script) : This Matlab script conducts two dimensional idealized test cases. In order to make changes in flow field, code must be modified.

A.2 Matlab Scripts for Three Dimensional Calculations

readvelodata.m(Function) : This Matlab function reads MSEAS data and puts it into path, and it reads velocity components at every time step from given ocean prediction data. The structure of this Matlab function is stated as follows.

$$[u, v, w, a] = \text{readvelodata}(x\text{gridnumber}, y\text{gridnumber}, z\text{gridnumber}, \text{time}, \text{speed}, \text{rec_num}, \text{ncid})$$

where *xgridnumber* is number of grid points in the cartesian x direction, *ygridnumber* is number of grid points in the cartesian y direction, *zgridnumber* is number of grid points in the cartesian z direction, *time* is number of ocean forecast step, *speed* is the speed of AUV, *ncid* is the name of ocean prediction data formatted as netcdf. The outputs of this functions are stated as follows. *u* is cartesian x component of the velocity field, *v* is the cartesian y component of the velocity field, *w* is the cartesian z component of the velocity field, *a* is the normal velocity field of the wave front.

vertface2obj.m (Function) : For visualization purposes, this function saves coordinates of vertices of faces as a Wavefront (.Obj) file. The structure of this Matlab function is stated as follows

$$\text{vertface2obj}(v, f, \text{name})$$

where *v* is a $N \times 3$ matrix of vertex coordinates, *f* is a $M \times 3$ matrix of vertex indices, and *fname* is the filename to save the obj file.

setdomain.m (Script) : This Matlab script initializes signed distance domain required for level set path planning

setoperators.m (Script) : This Matlab script initializes the differential operators and field forces matrices.

mseaspathplanning3d.m (Function) : This Matlab function is the main function that carries out the path planning calculations. It conducts numerical calculations and reinitialization of the signed distance field. The structure of this function is stated as follows.

mseaspathplanning3d(flowfield, xgridnumber, ygridnumber, zgridnumber, recnum, speed, start, target, saveobj)

where flow field is optional flow field structure, and by default it is input as "[]", xgridnumber is number of grid points in the cartesian x direction, ygridnumber is number of grid points in the cartesian y direction, zgridnumber is number of grid points in the cartesian z direction, *recnum* is the number ocean forecast step, start is the start point of underwater vehicle, target is the goal point of underwater vehicle, saveobj is the name of the data file which is saved for the visualization purposes.

savevtkfile.m (Script) : This script creates animations file directory, and calls vertface2obj function to create wavefront (.obj) data.

savevtkvector.m (Function) : savevtkvector.m function saves a 3-D vector of any size to filename in VTK format. X, Y and Z should be arrays of the same size, each storing speeds in the a single cartesian directions. The structure of this function is stated as follows

savevtkvector (readfile,filename)

where readfile is the name of dat file in which we save three dimensional velocity data, and filename is the name of vtk file we would like to save.

plotpath.m (Script) : This script plots the three dimensional paths. When this script is used, four subplot are seen on screen. Three of these plots are projections of three dimensional trajectory on to cartesian planes, and the fourth one is three dimensional plot.

PlotPath (XX,YY,ZZ) (Function) : PlotPath function shows the cartesian planes projections and three dimensional trajectory on the same plot window. The structure of PlotPath function is stated as follows.

PlotPath (XX,YY,ZZ)

where XX is cartesian x coordinate of the trajectory, YY is cartesian y coordinate of the trajectory, and ZZ is cartesian z coordinate of the trajectory.

Bibliography

- Adalsteinsson, D. and Sethian, J. (1995). A fast level set method for propagating interfaces. *Journal of computational physics*, 118(2):269–277.
- Agarwal, A. (2009). Statistical field estimation and scale estimation for complex coastal regions and archipelagos. Technical report, MASSACHUSETTS INST OF TECH CAMBRIDGE DEPT OF MECHANICAL ENGINEERING.
- Agarwal, A. and Lermusiaux, P. (2011). Statistical Field Estimation for Complex Coastal Regions and Archipelagos. *Submitted to Journal of Ocean Modelling*.
- Alton, K. and Mitchell, I. (2009). Fast marching methods for stationary Hamilton–Jacobi equations with axis-aligned anisotropy. *SIAM Journal on Numerical Analysis*, 47(1):363–385.
- Alvarez, A., Caiti, A., and Onken, R. (2004). Evolutionary path planning for autonomous underwater vehicles in a variable ocean. *Oceanic Engineering, IEEE Journal of*, 29(2):418–429.
- Ascher, U. and Petzold, L. (1998). *Computer methods for ordinary differential equations and differential-algebraic equations*, volume 61. Society for Industrial Mathematics.
- Botella, O. and Peyret, R. (1998). Benchmark spectral results on the lid-driven cavity flow. *Computers & Fluids*, 27(4):421–433.
- Bressan, A. and Piccoli, B. (2007). *Introduction to the mathematical theory of control*. American institute of mathematical sciences.
- Bretherton, F., Davis, R., and Fandry, C. (1976). A technique for objective analysis and design of oceanographic experiments applied to mode-73. *Deep-Sea Res*, 23(7):559–582.
- Bridson, R. (2003). *Computational aspects of dynamic surfaces*. PhD thesis, Citeseer.
- Bruckstein, A. (1988). On shape from shading. *Computer Vision, Graphics, and Image Processing*, 44(2):139–154.
- Carroll, K., McClaran, S., Nelson, E., Barnett, D., Friesen, D., and William, G. (1992). AUV path planning: an A* approach to path planning with consideration of

- variable vehicle speeds and multiple, overlapping, time-dependent exclusion zones. In *Autonomous Underwater Vehicle Technology, 1992. AUV'92., Proceedings of the 1992 Symposium on*, pages 79–84. IEEE.
- Cecil, T. and Marthaler, D. (2006). A variational approach to path planning in three dimensions using level set methods. *Journal of Computational Physics*, 211(1):179–197.
- Chopp, D. (1993). Computing minimal surfaces via level set curvature flow. *Journal of Computational Physics*, 106:77–77.
- Corbett, R. (2005). *Point-Based Level Sets and Progress Towards Unorganised Particle Based Fluids*. PhD thesis, The University of British Columbia.
- Courant, R., Isaacson, E., and Rees, M. (1952). On the solution of nonlinear hyperbolic differential equations by finite differences. *Communications on Pure and Applied Mathematics*, 5(3):243–255.
- Crandall, M., Ishii, H., Lions, P., and Society, A. M. (1992). *User's guide to viscosity solutions of second order partial differential equations*. American Mathematical Society.
- Crandall, M. and Lions, P. (1983). Viscosity solutions of Hamilton-Jacobi equations. *Transactions of the American Mathematical Society*, 277(1):1–42.
- Crandall, M. and Lions, P. (1984). Two approximations of solutions of Hamilton-Jacobi equations. *Mathematics of Computation*, 43(167):1–19.
- Cristiani, E. (2009). A fast marching method for Hamilton-Jacobi equations modeling monotone front propagations. *Journal of Scientific Computing*, 39(2):189–205.
- Dijkstra, E. (1959). A note on two problems in connexion with graphs. *Numerische mathematik*, 1(1):269–271.
- Dorst, L. and Trovato, K. (1988). Optimal path planning by cost wave propagation in metric configuration space. In *Society of Photo-Optical Instrumentation Engineers (SPIE) Conference Series*, volume 1007, page 186.
- Evans, J., Patrón, P., Smith, B., and Lane, D. (2008). Design and evaluation of a reactive and deliberative collision avoidance and escape architecture for autonomous robots. *Autonomous Robots*, 24(3):247–266.
- Fleming, W. and Soner, H. (2006). *Controlled Markov processes and viscosity solutions*. Springer.
- Garau, B., Alvarez, A., and Oliver, G. (2005). Path planning of autonomous underwater vehicles in current fields with complex spatial variability: an A* approach. In *Robotics and Automation, 2005. ICRA 2005. Proceedings of the 2005 IEEE International Conference on*, pages 194–198. IEEE.

- Giga, Y. (2006). *Surface evolution equations: A level set approach*. Birkhauser.
- Godunov, S. (1959). A difference method for numerical calculation of discontinuous solutions of the equations of hydrodynamics. *Matematicheskii Sbornik*, 89(3):271–306.
- Gout, C. and Guyader, C. (2006). Segmentation of complex geophysical structures with well data. *Computational Geosciences*, 10(4):361–372.
- Haley, P. and Lermusiaux, P. (2010). Multiscale two-way embedding schemes for free-surface primitive equations in the multidisciplinary simulation, estimation and assimilation system. *Ocean dynamics*, 60(6):1497–1537.
- Hassouna, M., Abdel-Hakim, A., and Farag, A. (2005). Robust robotic path planning using level sets. In *Image Processing, 2005. ICIP 2005. IEEE International Conference on*, volume 3, pages III–473. IEEE.
- Hoffman, J. (2001). *Numerical methods for engineers and scientists*. CRC.
- Houston, B., Nielsen, M., Batty, C., Nilsson, O., and Museth, K. (2006). Hierarchical level set: A compact and versatile deformable surface representation. *ACM Transactions on Graphics (TOG)*, 25(1):151–175.
- Inanc, T., Shadden, S., and Marsden, J. (2005). Optimal trajectory generation in ocean flows. In *Proceedings of the American Control Conference*, volume 1, page 674. Citeseer.
- Kanakakis, V. and Tsourveloudis, N. (2007). Evolutionary path planning and navigation of autonomous underwater vehicles. In *Control & Automation, 2007. MED'07. Mediterranean Conference on*, pages 1–6. IEEE.
- Kano, H., Egerstedt, M., Nakata, H., and Martin, C. (2003). B-splines and control theory. *Applied mathematics and computation*, 145(2-3):263–288.
- Ki, H., Mohanty, P., and Mazumder, J. (2001). Modelling of high-density laser-material interaction using fast level set method. *Journal of Physics D: Applied Physics*, 34:364.
- Kimmel, R. and Bruckstein, A. (1992). *Shape from shading via level sets*.
- Kimmel, R. and Bruckstein, A. (1993). Shape offsets via level sets. *Computer-Aided Design*, 25(3):154–162.
- Kimmel, R. and Sethian, J. (1998). Computing geodesic paths on manifolds. *Proceedings of the National Academy of Sciences*, 95(15):8431.
- Kimmel, R. and Sethian, J. (2001). Optimal algorithm for shape from shading and path planning. *Journal of Mathematical Imaging and Vision*, 14(3):237–244.

- Koenig, S., Likhachev, M., and Furcy, D. (2004). Lifelong planning A*. *Artificial Intelligence*, 155(1-2):93–146.
- Kruusmaa, M. (2003). Global navigation in dynamic environments using case-based reasoning. *Autonomous Robots*, 14(1):71–91.
- LaValle, S. (2006). *Planning algorithms*. Cambridge Univ Pr.
- Lermusiaux, P. (2006). Uncertainty estimation and prediction for interdisciplinary ocean dynamics. *Journal of Computational Physics*, 217(1):176–199.
- Lermusiaux, P. (2007). Adaptive modeling, adaptive data assimilation and adaptive sampling. *Physica D: Nonlinear Phenomena*, 230(1-2):172–196.
- Lermusiaux, P., Haley Jr, P., Leslie, W., Agarwal, A., Logutov, O., and Burton, L. (2011). Multiscale physical and biological dynamics in the philippine archipelago: Predictions and processes. *Oceanography*, 24(1):70–89.
- Lermusiaux, P., Xu, J., Chen, C., Jan, S., Chiu, L., and Yang, Y. (2010). Coupled Ocean–Acoustic Prediction of Transmission Loss in a Continental Shelfbreak Region: Predictive Skill, Uncertainty Quantification, and Dynamical Sensitivities. *Oceanic Engineering, IEEE Journal of*, 35(4):895–916.
- Losasso, F., Gibou, F., and Fedkiw, R. (2004). Simulating water and smoke with an octree data structure. In *ACM Transactions on Graphics (TOG)*, volume 23, pages 457–462. ACM.
- Malladi, R. and Sethian, J. (1996). Level set and fast marching methods in image processing and computer vision. In *Image Processing, 1996. Proceedings., International Conference on*, volume 1, pages 489–492. IEEE.
- Malladi, R., Sethian, J., and Vemuri, B. (1995). Shape modeling with front propagation: A level set approach. *Pattern Analysis and Machine Intelligence, IEEE Transactions on*, 17(2):158–175.
- Mulder, W., Osher, S., and Sethian, J. (1992). Computing interface motion in compressible gas dynamics. *Journal of Computational Physics*, 100(2):209–228.
- Nielsen, M. and Museth, K. (2006). Dynamic tubular grid: An efficient data structure and algorithms for high resolution level sets. *Journal of Scientific Computing*, 26(3):261–299.
- Osher, S. and Fedkiw, R. (2001). Level Set Methods: An Overview and Some Recent Results* 1. *Journal of Computational Physics*, 169(2):463–502.
- Osher, S. and Fedkiw, R. (2003). *Level set methods and dynamic implicit surfaces*. Springer Verlag.
- Osher, S. and Paragios, N. (2003). *Geometric level set methods in imaging, vision, and graphics*. Springer-Verlag New York Inc.

- Osher, S. and Sethian, J. (1988). Fronts propagating with curvature-dependent speed: algorithms based on Hamilton-Jacobi formulations. *Journal of computational physics*, 79(1):12–49.
- Paragios, N. and Deriche, R. (2002). Geodesic active regions and level set methods for supervised texture segmentation. *International Journal of Computer Vision*, 46(3):223–247.
- Parker, G., Wheeler-Kingshott, C., and Barker, G. (2002). Estimating distributed anatomical connectivity using fast marching methods and diffusion tensor imaging. *Medical Imaging, IEEE Transactions on*, 21(5):505–512.
- Petres, C., Pailhas, Y., Patron, P., Petillot, Y., Evans, J., and Lane, D. (2007). Path planning for autonomous underwater vehicles. *Robotics, IEEE Transactions on*, 23(2):331–341.
- Rouy, E. and Tourin, A. (1992). A viscosity solutions approach to shape-from-shading. *SIAM Journal on Numerical Analysis*, 29(3):867–884.
- Russo, G. and Smereka, P. (2000). A remark on computing distance functions. *Journal of Computational Physics*, 163(1):51–67.
- Sapsis, T. and Lermusiaux, P. (2009). Dynamically orthogonal field equations for continuous stochastic dynamical systems. *Physica D: Nonlinear Phenomena*, 238(23–24):2347–2360.
- Senatore, C. and Ross, S. (2008). Fuel-efficient navigation in complex flows. In *American Control Conference, 2008*, pages 1244–1248. IEEE.
- Sethian, J. (1996a). A fast marching level set method for monotonically advancing fronts. *Proceedings of the National Academy of Sciences of the United States of America*, 93(4):1591.
- Sethian, J. (1996b). *Level set methods: Evolving interfaces in geometry, fluid mechanics, computer vision, and materials science*, volume 1999. Cambridge University Press Cambridge:.
- Sethian, J. (1999). Fast marching methods. *SIAM review*, 41(2):199–235.
- Sethian, J. (2001). Evolution, implementation, and application of level set and fast marching methods for advancing fronts. *Journal of Computational Physics*, 169(2):503–555.
- Sethian, J. and Vladimirovsky, A. (2000). Fast methods for the Eikonal and related Hamilton–Jacobi equations on unstructured meshes. *Proceedings of the National Academy of Sciences of the United States of America*, 97(11):5699.
- Sethian, J. and Vladimirovsky, A. (2004). Ordered upwind methods for static Hamilton–Jacobi equations: theory and algorithms. *SIAM Journal on Numerical Analysis*, pages 325–363.

- Smith, R., Kelly, J., Chao, Y., Jones, B., and Sukhatme, G. (2010). Towards improvement of autonomous glider navigation accuracy through the use of regional ocean models. In *Proceedings of the 29th International Conference on Ocean, Offshore and Arctic Engineering*, pages 597–606. ASME-American Society Mechanical Engineering.
- Soner, H. and Touzi, N. (2002). A stochastic representation for the level set equations. *Communications in Partial Differential Equations*, 27(9):2031–2053.
- Soullignac, M., Taillibert, P., and Rueher, M. (2008). Adapting the wavefront expansion in presence of strong currents. In *Robotics and Automation, 2008. ICRA 2008. IEEE International Conference on*, pages 1352–1358. IEEE.
- Soullignac, M., Taillibert, P., and Rueher, M. (2009). Time-minimal path planning in dynamic current fields. In *Robotics and Automation, 2009. ICRA '09. IEEE International Conference on*, pages 2473–2479. IEEE.
- Strain, J. (1999). Tree methods for moving interfaces* 1. *Journal of Computational Physics*, 151(2):616–648.
- Sussman, M. and Fatemi, E. (1999). An efficient, interface-preserving level set redistancing algorithm and its application to interfacial incompressible fluid flow. *SIAM Journal on Scientific Computing*, 20(4):1165–1191.
- Sussman, M. and Puckett, E. (2000). A coupled level set and volume-of-fluid method for computing 3D and axisymmetric incompressible two-phase flows. *Journal of Computational Physics*, 162(2):301–337.
- Sussman, M., Smereka, P., and Osher, S. (1994). *A level set approach for computing solutions to incompressible two-phase flow*. Dept. of Mathematics, University of California, Los Angeles.
- Tan, C., Sutton, R., and Chudley, J. (2004). An incremental stochastic motion planning technique for autonomous underwater vehicles. *Proceedings IFAC CAMS, 20004*:483–488.
- Tsitsiklis, J. (1994). Efficient algorithms for globally optimal trajectories. In *Decision and Control, 1994., Proceedings of the 33rd IEEE Conference on*, volume 2, pages 1368–1373. IEEE.
- Tsitsiklis, J. (1995). Efficient algorithms for globally optimal trajectories. *Automatic Control, IEEE Transactions on*, 40(9):1528–1538.
- Vasudevan, C. and Ganesan, K. (1996). Case-based path planning for autonomous underwater vehicles. *Autonomous Robots*, 3(2):79–89.
- Whitaker, R. (1998). A level-set approach to 3d reconstruction from range data. *International Journal of Computer Vision*, 29(3):203–231.

- Witt, J. and Dunbabin, M. (2008). Go with the flow: Optimal AUV path planning in coastal environments. In *Proceedings of the Australasian Conference on Robotics and Automation*.
- Xu, B., Stilwell, D., and Kurdila, A. (2009). Efficient computation of level sets for path planning. In *Intelligent Robots and Systems, 2009. IROS 2009. IEEE/RSJ International Conference on*, pages 4414–4419. IEEE.
- Yang, G. and Zhang, R. (2009). Path Planning of AUV in Turbulent Ocean Environments Used Adapted Inertia-Weight PSO. In *2009 Fifth International Conference on Natural Computation*, pages 299–302. IEEE.
- Zhang, W., Inane, T., Ober-Blobaum, S., and Marsden, J. (2008). Optimal trajectory generation for a glider in time-varying 2D ocean flows B-spline model. In *Robotics and Automation, 2008. ICRA 2008. IEEE International Conference on*, pages 1083–1088. IEEE.
- Zhao, H., Chan, T., Merriman, B., and Osher, S. (1996). A variational level set approach to multiphase motion. *Journal of computational physics*, 127(1):179–195.